Universitat de Barcelona

Facultat de Biologia

Dpt de Bioquímica i Biologia Molecular

Funciones *in vivo* del regulador transcripcional HNF1α (MODY3)

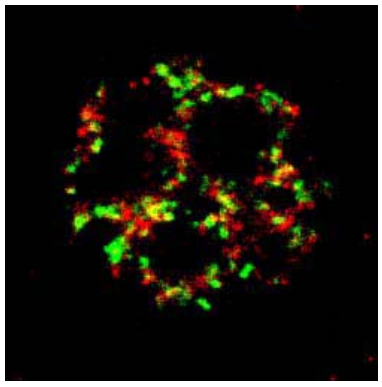

Reina Fdez de Luco, 2007

RESULTADOS

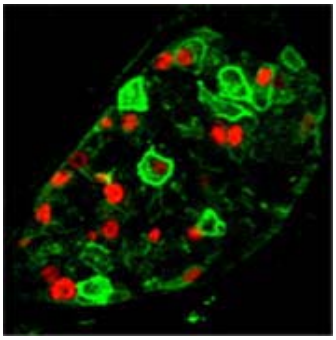

A conditional model reveals that induction of Hepatocyte Nuclear Factor-1α in *Hnf1α*-null mutant β-cells can activate silenced genes postnatally, whereas overexpression is deleterious.

RF Luco, MA Maestro, N del Pozo, WM Philbrick, P Perez de la Ossa and J Ferrer, 2006.

Diabetes, vol.55 p2202-2209

Mutaciones en heterocigosidad del factor de transcripción HNF1α causan diabetes tipo MODY3 en humanos, evidenciando la importancia de este factor para el correcto funcionamiento de la célula beta. Sin embargo, importantes cuestiones acerca de la función *in vivo* de HNF1α en un contexto celular son aún desconocidas. No se sabe si esta función es autónoma celular, si está restringida a algún momento del desarrollo de la célula beta o si cantidades elevadas de HNF1α causan igualmente disfunción de célula beta. Estas tres preguntas son de vital importancia para el desarrollo de terapias génicas de rescate de la función de HNF1α, o para el establecimiento de protocolos *in vitro* de diferenciación de células beta.

Para responder a estas cuestiones, hemos desarrollado en el laboratorio un modelo transgénico inducible y específico de tejido que permite expresar HNF1α en el momento del desarrollo que deseemos y selectivamente en células beta de ratones que tienen inactivado el locus HNF1α endógeno. Este sistema sobreexpresa HNF1α, de manera que podemos estudiar la repercusión de la dosis génica en la función de HNF1α en la célula beta.

Las principales conclusiones del estudio son:

1) Los niveles de expresión de HNF1α en célula beta son críticos para su correcta función.

Mientras que la reducción de la función HNF1α es deletérea para la célula beta y causa MODY3, la sobreexpresión de HNF1α induce muerte celular e inhibe la proliferación, causando a largo plazo una reducción de la masa de célula beta que acaba derivando en diabetes

2) HNF1α tiene una función autónoma celular en la célula beta

Debido al fenotipo deletéreo de la sobreexpresión de HNF1α, no podemos mejorar el fenotipo diabético en ratones deficientes para HNF1α en los que reexpresamos HNF1α exclusivamente en célula beta. Sin embargo, existe heterogeneidad en los niveles de sobreexpresión de HNF1α transgénico, de manera que tanto *in vivo* como en islotes reinducidos en cultivo, conseguimos recuperar en parte la expresión de algunas dianas de HNF1α, como Glut2, sólo en aquellas células que expresan HNF1α a niveles casi fisiológicos,. Así pues, parece que la función reguladora transcripcional de HNF1α en célula beta posee autonomía celular.

3) La función de HNF1α no está restringida a una ventana temprana del desarrollo de la célula beta.

A diferencia de los estudios de reexpresión de HNF1α en hepatocitos adultos (Viollet et al, 2001), podemos recuperar la expresión de algunas dianas de HNF1α cuando inducimos la expresión de HNF1α en células beta deficientes para HNF1α (*Hnf1α*$^{-/-}$) postnatalmente, tanto *in vivo* como *ex vivo*.

Este estudio tiene repercusiones en el desarrollo de terapias génicas y de protocolos de diferenciación in vitro de células beta. Pero también llama la atención sobre el peligro de sobreexpresar factores de transcripción para el estudio de su función, así como el uso de modelos de sobreexpresión de mutantes dominantes negativos como sustitutos de los modelos genoanulados.

LINK:
http://diabetes.diabetesjournals.org/cgi/content/full/55/8/2202

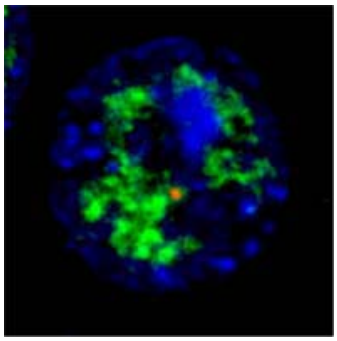

Hnf1α repositions its genomic targets to subnuclear histone code domains

RF Luco, MA Maestro and J Ferrer, 2006

en revisión en Journal of Cell Biology

La regulación de la transcripción está integrada por varios niveles jerárquicos. Basándonos en el modelo deficiente para el factor de transcripción HNF1α, *Hnf1α*$^{-/-}$, hemos explorado la relación entre la regulación de la transcripción al nivel local de cromatina y al nivel espacial de núcleo integradas por un activador, HNF1α

Las principales conclusiones que derivan de este trabajo son:

1) HNF1α induce modificaciones de histona que alteran la conformación de la cromatina

HNF1α induce la acetilación y la metilación de H3-Lys4 de las colas de histona de las zonas promotoras. En su ausencia, los genes diana están hipoacetilados, metilados en H3-Lys27 y la cromatina está más compactada.

2) Las modificaciones de histonas se distribuyen en el núcleo formando subdominios discretos.

La metilación en H3-Lys27 (H3-Lys27me3) forma un dominio generalmente excluyente con dominios rico en H3-Lys9me3, H3-Lys4me2 y RNA polimerasa II. La distribución de H3-Lys27me3 es principalmente periférica, mientras que los dominios ricos en RNA polimerasa II tienden a situarse en el interior del núcleo.

3) El propio HNF1α está distribuido en dominios discretos funcionales.

HNF1α colocaliza con dominios ricos en RNA polimerasa II y H3-Lys4me pero no H3-Lys27me. Los genes activos se localizan con mayor frecuencia en dominios ricos en HNF1α y RNA polimerasa II.

4) HNF1α induce el reposicionamiento localizado de sus loci diana a dominios nucleares ricos en determinadas modificaciones de histona, en concordancia con las modificaciones inducidas localmente.

Los genes activos dependientes de HNF1α se localizan en dominios ricos en RNA polimerasa II y H3-Lys4me2. En ausencia de HNF1α, estos genes están inactivos y tienden a reposicionarse en dominios ricos en H3-Lys27me3 y pobres en RNA polimerasa II. Este reposicionamiento es dependiente de activador y está altamente localizado afectando sólo al locus regulado por HNF1α.

Este trabajo tiene implicaciones en la comprensión del defecto celular de MODY3, ya que indica que esta enfermedad se caracteriza por una deslocalización nuclear de genes importantes para la función diferenciada de la célula beta. Por otra parte, también tiene implicaciones en nuestra comprensión de la función integrada de un factor de transcripción. Se muestra un vínculo entre la regulación a nivel de la unión específica a DNA de un activador (HNF1α), la inducción de cambios locales a nivel de la cromatina y el reposicionamiento de los genes diana a dominios

subnucleares ricos en las modificaciones de histona inducidas localmente. Estos estudios demuestran por primera vez en un modelo genético *in vivo* que el reposicionamiento génico es un fenómeno altamente localizado y dependiente de un activador, y que existe una representación funcional en el espacio nuclear de las modificaciones de cromatina inducidas localmente.

Title:

Hnf1α repositions its genomic targets to subnuclear histone code domains

Short running title:

A histone code in nuclear space

Authors:

Reini F. Luco[1,2], Miguel A. Maestro[1,2] and Jorge Ferrer[1,3]

Affiliations:

[1]Genomic Programming of Beta-cells Laboratory. Institut d´Investigacions August Pi i Sunyer, Endocrinology, Hospital Clinic de Barcelona, Villarroel 170 08036, Barcelona, Spain

[2]These authors contributed equally to this work

[3]Correspondence should be addressed to J.Ferrer (e-mail:jferrer@clinic.ub.es)

Number of characters:

Title: 63 characters

Running title: 26 characters

Abstract: 172 words

Manuscript: 29.680 characters

Abstract:

Covalent modifications of histone tails are instrumental in transcriptional regulation. Transcription is also associated with the positioning of genes within the nucleus. We have studied the relationship between these two layers of regulation using mice lacking Hnf1α, a transcriptional activator involved in human monogenic diabetes (MODY3). In *Hnf1α*$^{-/-}$ primary β-cells and hepatocytes, inactive Hnf1α-target genes exhibit reduced methylated H3-Lys4 and increased trimethylated histone H3-Lys27. We demonstrate that these histone modifications are enriched in separate subnuclear domains, and that Hnf1α is preferentially located in domains enriched in both methylated H3-Lys4 and RNA polymerase II. Remarkably, in wild type cells Hnf1α-dependent targets are preferentially positioned in such active subnuclear domains, while in *Hnf1α*$^{-/-}$ cells they are located in domains enriched in methylated H3-Lys27. The analysis of adjacent genomic loci shows that Hnf1α-dependent positioning is locus-selective rather than the reflection of a broad chromosomal territory reconfiguration. Thus, the transcriptional activator Hnf1α promotes site-specific histone modifications, and concomitantly repositions genomic targets to subnuclear domains defined by the content of both RNA polymerase II and histone modifications.

Introduction

The control of gene transcription is a complex process that is integrated at multiple levels (Kosak and Groudine, 2004;van Driel et al., 2003). One critical step is the recognition of nucleotide sequences in the vicinity of genes by DNA binding factors that elicit transcriptional activation or repression (Kadonaga, 2004). Another level is provided by the remodeling of chromatin structure and the covalent modification of nucleosomal histone tails (Felsenfeld and Groudine, 2003). These two levels of regulation are linked by numerous observations that DNA binding factors recruit chromatin remodeling and histone modifying activities near the binding sites (Kadonaga, 2004;Kosak and Groudine, 2004;Soutoglou et al., 2001;van Driel et al., 2003).

Post-translational histone modifications are thought to act by altering chromatin structure and enabling the recruitment of additional regulatory proteins (Felsenfeld and Groudine, 2003;Jenuwein and Allis, 2001;Turner, 2002). Diverse histone modifications have been associated with transcriptional state. For example, enzymatic acetylation or deacetylation of histone H3 and H4 tails has been linked to gene activation and silencing, respectively (Felsenfeld and Groudine, 2003;Jenuwein and Allis, 2001;Schubeler et al., 2004;Turner, 2002). The methylation of H3-Lys4 at gene promoters has been tightly linked to gene activity (Santos-Rosa et al., 2002;Schubeler et al., 2004;Strahl et al., 1999), whereas transcriptional silencing correlates with either H3-Lys9 or H3-Lys27 hypermethylation (Cao et al., 2002;Mager et al., 2003;Martens et al., 2005;Peters et al., 2003;Plath et al., 2003). In particular, trimethylated H3-Lys9 (H3-Lys9me3) is enriched at pericentromeric repeats forming constitutive heterochromatin (Martens et al., 2005;Peters et al., 2003), while trimethylated

H3-Lys27 (H3-Lys27me3) has been linked to other forms of silenced chromatin, including chromosome X facultative heterochromatin, imprinted loci, and epigenetic silencing of homeobox gene clusters (Cao et al., 2002;Mager et al., 2003;Plath et al., 2003).

It has recently become apparent that the positioning of gene loci within the three dimensional structure of the nucleus may provide a further level of regulation (reviewed in (Chakalova et al., 2005;Cremer and Cremer, 2001;Kosak and Groudine, 2004). For example, gene transcription has been proposed to occur near the surface of chromosomal condensations, in the so called interchromatin compartment (Cremer and Cremer, 2001;Verschure et al., 1999). Gene activation has also been linked to selective looping of loci away from chromosomal territories (Chambeyron and Bickmore, 2004), and to an increased likelihood that a locus intermingles with heterologous chromosomal territories (Branco and Pombo, 2006). There is now evidence that transcribing genes colocalize with nuclear domains that are visibly enriched in RNA polymerase II (Osborne et al., 2004;Ragoczy et al., 2006;Wansink et al., 1993). On the other hand, inactive genes are frequently positioned in more peripheral parts of the nucleus (Gasser, 2001;Kosak et al., 2002;Kosak and Groudine, 2004;Zink et al., 2004), while repositioning to centromeric regions has been shown in several hematopoietic genes during differentiation-related silencing, as well as in the silenced brown locus mutation in Drosophila (Brown et al., 1997;Brown et al., 1999;Brown et al., 2001;Cobb et al., 2000;Dernburg et al., 1996;Francastel et al., 2001;Merkenschlager et al., 2004;Su et al., 2004). However, the mechanisms that govern locus repositioning, and the possible interplay with more established levels of transcriptional control, such as the site-

specific modification of histone tails, remain largely unknown. Moreover, it is not clear yet to what extent gene repositioning can be activator-dependent, or if by contrast it may be primarily influenced by factors related to the location of broad chromosomal domains, as suggested by the observation that gene-rich regions tend to locate outside of their chromosomal territories irrespective of gene activity (Gilbert et al., 2004).

In the current study, we have explored the relationship between activator-dependent histone modifications and gene positioning in the interphase nucleus of primary cells. This was addressed in a model of deficiency for the transcriptional activator Hnf1α (also known as Tcf1). Hnf1α is a homeodomain protein encoded by the gene implicated in MODY3, the major cause of human monogenic diabetes (Yamagata et al., 1996). Knock-out mice have shown that Hnf1α is dispensable for organogenesis, but is essential for the activity of several genes involved in differentiated functions of liver, kidney, and pancreatic beta-cells (Boj et al., 2001;Ferrer, 2002;Lee et al., 1998;Pontoglio et al., 1996;Pontoglio et al., 1998). Using immuno-FISH, we have studied the subnuclear position of Hnf1α-dependent target genes in primary hepatocytes and islet-cells from Hnf1α-null mutant and control mice. The same analysis was carried out for several Hnf1α-independent loci. This model enabled us to ascribe observed changes to the presence or absence of an activator, thus minimizing the confounding effects of comparing cell-types or developmental stages with profoundly different chromosomal configurations (Bolzer et al., 2005;Parada et al., 2004), while at the same time avoiding the use of transformed cell lines and artificial overexpression systems.

The results indicate that Hnf1α-dependent transcription correlates with the repositioning of loci to domains enriched in RNA polymerase II, thus providing a direct genetic demonstration that this phenomenon is activator-dependent. We show that Hnf1α-dependent repositioning is locus-selective rather than a reflection of a broad reconfiguration of chromosomal territories. The studies also reveal that Hnf1α-dependent repositioning to RNA polymerase II foci entails the relocation between compartments that differ in their histone modification content. Hnf1α is thus shown to not solely induce local chromatin modifications, but to increase the probability that targets are repositioned from a repressive to a transcriptionally active chromatin domain in nuclear space. These findings add novel insights to our understanding of the *in vivo* function of a transcriptional activator, and for the first time link subnuclear gene repositioning to a human transcriptional disease.

Results

Hnf1α alters the methylated histone pattern and chromatin compaction of its target genes. Earlier studies showed that Hnf1α-dependent transcription is dependent on the recruitment of histone acetyltransferases and the local acetylation of nucleosomal histones (Parrizas et al., 2001;Soutoglou et al., 2001). We have now examined the methylation state of histone H3 in target genes. For this analysis we selected the most profoundly downregulated genes identified in expression profiling experiments of *Hnf1α*$^{-/-}$ hepatocytes (*Afm*, *Cyp2j5* and *Pah*) and islets (*Kif12*) , all of which behave as cell-specific targets in their respective cell-types (**Fig.1A, B)**. The four genes contain evolutionary

conserved high-affinity Hnf1 binding sites in their promoter region, and were experimentally shown to be directly bound by Hnf1α (**Fig.1 C**, not shown).

As shown in **Fig.1D,M,** dimethylated H3-Lys4 (H3-Lys4me2) was reduced in the 5' flanking chromatin of such genes in *Hnf1α*-deficient hepatocytes, while no changes where observed in control genes (**Fig. 1E**).

Surprisingly, H3-Lys9me3, an established repressive mark associated with constitutive heterochromatin (Martens et al., 2005;Peters et al., 2003), was not increased in these genes in *Hnf1α*$^{-/-}$ hepatocytes (**Fig.1F**), but was readily detected in minor satellite positive control sequences (**Fig.1L**). A 3.5 to 5-fold increase in dimethylated H3-Lys9 was nevertheless observed in inactive targets in *Hnf1α*$^{-/-}$ cells (data not shown).

We next assessed the methylation state of Lys27 in histone H3, a modification previously found to be enriched in several forms of facultative heterochromatin (Cao et al., 2002;Mager et al., 2003;Plath et al., 2003). Increased H3-Lys27me3 was detected in Hnf1α-dependent targets in *Hnf1α*$^{-/-}$ hepatocytes (*Afm, Cyp2j5* and *Pah*), but not in control genes (*Tbp, Nanog* and *Ly9*) (**Fig.1H-K**). This represented primarily trimethylated H3-Lys27, as it was detected with antisera selectively recognizing H3-Lys27me2,3 and H3-Lys27me3, but not H3-Lys27me2 (**Fig.1I,K,M** and not shown). Interestingly, increased H3-Lys27me2,3 was spread throughout the *Cyp2j5* locus, rather than being circumscribed to discrete segments (**Fig.1M**).

General DNAse I sensitivity studies revealed reduced degradation of *Cyp2j5* chromatin in *Hnf1α*$^{-/-}$ vs. *Hnf1α*$^{+/+}$ hepatocytes, whereas no differences were observed between genotypes for the control gene *Actb* (**Fig.1N**). Thus, in genes that are inactive due to Hnf1α-deficiency, there is a switch from an active

open chromatin conformation enriched in methylated H3-Lys4, to a repressed more compacted state enriched in tri-methylated H3-Lys27.

Different forms of methylated histone H3 are distributed non-randomly in nuclear space. To explore the possible relationship between gene activity, site-specific histone modifications, and nuclear organization, we next assessed whether histone modifications are non-randomly distributed in nuclei from primary hepatocytes and pancreatic islet-cells(the vast majority of which are quiescent under normal conditions). We used RNA polymerase II as a landmark, because previous studies indicate it is enriched in transcriptionally active nuclear domains (Iborra et al., 1996;Osborne et al., 2004;Ragoczy et al., 2006;Wansink et al., 1993). Interestingly, RNA polymerase II domains colocalized more frequently with regions that are strongly enriched in the histone covalent modification associated with transcriptional activity, H3-Lys4me2 (62% ± 1), as compared to marks associated with gene silencing, H3-Lys9me3 (6% ± 0) and Lys27me3 (17% ± 1) ($p<0.001$ for the two comparisons) (**Fig.2A-I and Supplementary video.1-3**). H3-Lys27me3-rich domains in turn exhibited only limited colocalization with domains enriched in H3-Lys4me2 (20% ± 2) (**Fig.2J-L**), but frequently overlapped with with H3-Lys9me2-rich zones (47% ± 1) (**Supplementary Fig.1A-C**). H3-Lys27me3-rich domains also showed some overlap with other repressive marks such as H3-Lys27me2 (37% ± 1)and H3-Lys9me3 (36% ± 1), although there was no obvious colocalization with strong H3-Lys9me3-stained pericentric foci (**Supplementary Fig.1A-I**).

Interestingly, in addition to being markedly enriched in Barr bodies of female cells (Plath et al., 2003), H3-Lys27me3 was clearly enriched in a more

peripheral portion of nuclear space, as well as in the perinucleolar region in both hepatocytes and pancreatic islet-cells (see examples in **Fig.2G,J, Fig.4C,D, Fig.5C,D, Supplementary Fig.1** and **Supplementary video.3,5**). In contrast, RNA polymerase II-rich domains occupied more central regions of nuclear space (**Fig.2A,G, Fig.4C,D, Fig.5C,D, Supplementary Fig.1M,P** and **Supplementary video.3**). This is of interest in light of previous results correlating gene silencing with positioning in the nuclear periphery (Gasser, 2001;Kosak et al., 2002;Kosak and Groudine, 2004;Zink et al., 2004).

These findings were independent of the fixative used and were confirmed with different H3-Lys27me3 antibodies (**Supplementary Fig.1J-R**). Of note, the H3-Lys27me3 immunostaining pattern was distinct from that of histone H3 and other modifications including H3-Lys4me2, H3-Lys9me3, H3-Lys27me1, and H3-Lys27me2, indicating that it does not merely reflect chromatin density (**Fig.2J-L, Supplementary Fig.1D-I** and not shown). These results are largely consistent with a recent study that describes nuclear patterns of histone modification (Zinner et al., 2006), but importantly extend it showing that H3-Lys4me2 exhibits preferential nuclear colocalization with RNA polymerase II, while H3-Lys27me3 conforms a nuclear domain that is distinct from regions enriched in H3-Lys9me3, H3-Lys4me2 and RNA polymerase II.

Hnf1α is preferentially located in subnuclear domains enriched in RNA polymerase II and H3-Lys4me2. We next assessed if Hnf1α protein partitions non-randomly amongst such histone modification subnuclear domains. Dual immunostaining studies revealed that Hnf1α-enriched pixels colocalized more frequently with domains enriched in RNA polymerase II and H3-Lys4me2

compared to domains enriched in H3-Lys27me3 (50% ± 4 and 44% ± 0 vs. 22% ± 0, respectively; p<0.001 for the two comparisons) (**Fig.3).** 3D reconstructions of such dual immunostainings suggested that, like RNA polymerase II, Hnf1α-rich regions are clearly located in a more central position relative to H3-Lys27me3-rich domains (**Supplementary video.4-5**). Importantly, this subnuclear Hnf1α pattern is specific, as it was observed using alternate fixation procedures, but not in *Hnf1α*$^{-/-}$ cells using identical conditions (**Supplementary Fig.2**). These findings suggested that there may be a compartmentalization of Hnf1α function within the nucleus.

Hnf1α induces locus repositioning between histone methylation subnuclear domains. We next tested if Hnf1α-dependent gene activity is associated with relocation among histone modification and RNA polymerase II domains. This was carried out with immuno-FISH, allowing us to compare the relative enrichment of histone modifications and RNA polymerase II in Hnf1α-dependent loci of control vs. null-mutant nuclei (**Fig.4A-D** and **Fig.5A-D**). As shown in **Supplementary Fig.1P-R,** the compartmentalization of histone marks was conserved after the immuno-FISH procedure. Furthermore, the overlapping patterns of histone mark and RNA polymerase II enrichment did not differ in control vs. null-mutant nuclei (data not shown).

In several instances, gene silencing has been associated with relocation to constitutive heterochromatic domains enriched in satellite repeat sequences (Brown et al., 1997;Brown et al., 1999;Brown et al., 2001;Cobb et al., 2000;Dernburg et al., 1996;Francastel et al., 2001;Merkenschlager et al., 2004;Su et al., 2004). In mice H3-Lys9me3 is conspicuously enriched in

pericentromeric regions (Martens et al., 2005;Peters et al., 2003), and this was confirmed in our conditions using the DNA marker TOPRO-3 (data not shown). However, Hnf1α-targets that are inactive in mutant hepatocytes (*Cyp2j5*) and islets (*Kif12*) did not relocalize to H3-Lys9me3-enriched domains (**Fig.4J** and not shown).

In sharp contrast, inactive Hnf1α-targets *Cyp2j5* and *Kif12* repositioned to nuclear domains enriched in H3-Lys27me3 in *Hnf1α*-deficient cells (**Fig.4K** and **Fig.5I)**. To verify the specificity of this effect, 4 control loci were examined (*Hnf1β, Ly9, Actb* and *Nanog*), none of which showed this pattern (**Fig.4F, Fig.5E** and **Supplementary Fig.3)**. Hnf1α-dependent expression of *Cyp2j5* and *Kif12* loci also strongly correlated with repositioning to both H3-Lys4me2 and RNA polymerase II-enriched nuclear regions (**Fig.4L,M** and **Fig.5J,K**).

The ability to simultaneously image two protein marks at each locus allowed us to more accurately assess the extent to which loci repositioned to domains enriched in opposed marks. The H3-Lys27me3/RNA polymerase II signal intensity ratio measured in individual *Cyp2j5* and *Kif12* alleles was thus found to be 8- and 2.3- fold higher in *Hnf1$\alpha^{-/-}$* vs. *Hnf1$\alpha^{+/+}$* cells, respectively, yet remained unaltered in control loci (**Fig.4I,N, Fig.5H,L** and **Supplementary Fig.3).** We furthermore classified loci in 4 categories, according to whether or not they were located in domains enriched in either the histone modification or RNA polymerase II (**Fig.4O-T** and **Fig.5M-P)**. This revealed that in null-mutant cells, *Hnf1α*-dependent genes *Cyp2j5* and *Kif12* were located in domains enriched in H3-Lys27me3 but not RNA polymerase II 2.6 and 3.3 times more frequently than expected, respectively **(Fig.4S** and **Fig.5O)**. Importantly, this did not reflect solely delocalization from RNA polymerase II-rich domains in null-

mutant cells, as the two genes were not more frequently found in domains lacking enrichment of both H3-Lys27me3 and RNA polymerase II **(Fig.4S** and **Fig.5O)**. Consistent with enrichment in H3-Lys27me3 but not H3-Lys9me3, *Cyp2j5* and *Kif12* alleles in *Hnf1*$\alpha^{-/-}$ cells were more frequently located in domains lacking enrichment of both RNA polymerase II and H3-Lys9me3 (**Fig.4R** and not shown). Finally, *Cyp2j5* and *Kif12* alleles in *Hnf1*$\alpha^{-/-}$ cells were respectively located 2 and 1.6 times more frequently than in controls in domains that lacked enrichment in both RNA polymerase II and H3-Lys4me2 (**Fig.4T** and **Fig.5P**). Importantly, these results were independent of the threshold used in the analysis (see methods), and were not observed in four control genes (**Fig.4O-T, Fig.5M-N** and not shown).

Control loci in this study are chosen because their gene activity is Hnf1α-independent, but they are not intended for interlocus comparisons in wild type cells, because none of the probes contains exclusively active or inactive genes (**Supplementary Table 2**). Nonetheless, loci containing several active transcriptional units (*Actb*, *Cyp2j5* and *Afm*) localized more frequently in Hnf1α and RNA polymerase II-rich regions than a control inactive gene locus (*Ly9*), further supporting that Hnf1α is preferentially compartmentalized in active nuclear domains (**Supplementary Fig.4**).

Hnf1α-dependent repositioning is a localized phenomenon. We next attempted to define the spatial resolution of Hnf1α-dependent repositioning within the limits of confocal light microscopy. We thus performed two-color DNA FISH using two contiguous BACs, named 68H9 and 114C9, located telomeric to the *Cyp2j5* locus (**Fig.6A**). The head-tail distances between *Cyp2j5* vs. 68H9

and 68H9 vs. 114C9 were 22 and 24 Kb, respectively (**Fig.6A**). Remarkably, despite their proximity, *Cyp2j5* and 68H9 clones could be clearly separated by dual FISH analysis in 65% of alleles, thus enabling to test whether BACs in the vicinity of *Cyp2j5* also repositioned with respect to subnuclear domains in *Hnf1*$\alpha^{-/-}$ cells (**Fig.6B,C**). The results showed that neither 68H9 nor 114C9 were differentially distributed with respect to RNA polymerase II or histone marks in *Hnf1*$\alpha^{-/-}$ vs. *Hnf1*$\alpha^{+/+}$ cells (**Fig.6D,E**). This result indicated that Hnf1α-dependent repositioning of *Cyp2J5* amongst such domains is a localized phenomenon.

We next sought to determine if Hnf1α-dependent repositioning can be elicited relative to a reference that is independent of the pattern of distribution of histone marks and RNA polymerase II. The two telomeric clones (68H9 and 114C9) map to a genomic sequence that appears to be completely devoid of transcriptional activity. In wild type cells, the average distance between *Cyp2j5* and 68H9 loci was 0.36 μm ± 0.02, whereas the distance between 68H9 and 114C9 was 0.27 μm ± 0.02 ($p<0.001$), in keeping with a more compact configuration of the transcriptionally inactive 68H9-114C9 region **(Fig.6F)**. Remarkably, in *Hnf1*$\alpha^{-/-}$ hepatocytes the transcriptionally inactive *Cyp2j5* locus was now located at a significantly shorter distance from the 68H9 locus (0.28 μm ± 0.02, $p<0.01$; **Fig.6F)**. Indeed, the distance between *Cyp2j5* and 68H9 vs. 68H9 and 114C9 no longer differed in *Hnf1*$\alpha^{-/-}$ hepatocytes **(Fig.6F).** Thus, the presence of Hnf1α modifies the position of *Cyp2j5* with respect to neighbouring chromosomal regions. These findings provide a direct verification of Hnf1α-dependent target repositioning independently of subnuclear histone enrichment

patterns, and indicate that it is locus-selective rather than secondary to a non-specific broad chromosomal reconfiguration in *Hnf1*$\alpha^{-/-}$ cells.

In summary, *Hnf1*α-dependent loci reposition from subnuclear domains enriched in H3-Lys27me3 in *Hnf1*$\alpha^{-/-}$ cells to active domains enriched in Hnf1α, RNA polymerase II, and H3-Lys4me2 in *Hnf1*$\alpha^{+/+}$ cells. This effect is specific for *Hnf1*α-dependent loci inasmuch as it does not occur in two adjacent genomic regions and four *Hnf1*α-independent distant loci.

Discussion

We have shown that the transcriptional activator Hnf1α alters the covalent modification pattern of target nucleosomes, and at the same time causes the relocation of target loci to subnuclear domains enriched in concordant histone modification enrichment patterns. This was shown using a genetic model that enabled us to directly test the effects of a transcriptional activator in primary differentiated cells, as opposed to relating gene transcription with position in different cell types or developmental stages with potentially different nuclear architectures (Bolzer et al., 2005;Parada et al., 2004;Ragoczy et al., 2006).

The analysis of numerous control loci allowed us to conclude that the spatial changes described here are specific for two genomic regions that are transcriptionally dependent on Hnf1α. Furthermore, the disparity in the behavior of adjacent chromosomal regions indicates that our observations truly reflect the selective repositioning of a locus, rather than a broadly altered chromosomal territory configuration or altered subnuclear organization of histone mark or RNA Polymerase II enrichment patterns in knock-out cells. However, our experimental procedure does not allow us to determine the exact extension of chromatin domains that undergo Hnf1α-dependent relocation, which may well be smaller than the resolution of optical microscopy. In this regard, it is worth noting that BAC probes used to detect Hnf1α-target genes inevitably contain Hnf1α-independent loci that evidently influence the final outcome of our analysis. Furthermore, it is plausible that active loci may reposition intermittently to active nuclear domains, in analogy to the notion that transcription is a discontinuous process (Osborne et al., 2004;Wijgerde et al., 1995). These

considerations are likely to contribute to the lack of absolute correspondence of locus positioning in active/inactive subnuclear domains, and suggest that Hnf1α-dependent relocation may be more pronounced than documented in this study.

Earlier studies have linked the function of other sequence specific-DNA binding proteins such as Ikaros and NF-E2p18 with locus repositioning (Brown et al., 1997;Cobb et al., 2000;Francastel et al., 2001). In such examples repressor-mediated repositioning of silenced loci to pericentromeric compartments is observed during active developmentally regulated settings. This clearly represents a different paradigm from the current analysis where silencing results from the sheer lack of an activator and does not lead to association with pericentromeric chromatin. None the less, in the aggregate such findings suggest that the relocation of transcriptional target loci may be a general function of sequence-specific DNA binding transcriptional regulators.

The model we propose to summarize current and previous findings is that binding to target loci by the activator Hnf1α causes local histone tail hyperacetylation, increased methylated H3-Lys4, chromatin decondensation, and prevention of methylated H3-Lys27 (Parrizas et al., 2001;Pontoglio et al., 1997;Soutoglou et al., 2001). H3-Lys27 methylation thus appears to represent a default state, consistent with genetic studies in Drosophila showing that Trithorax H3-Lys4 methyltransferase suppresses default methylated H3-Lys27-mediated gene silencing (Klymenko and Muller, 2004). Concomitant with these local changes, Hnf1α binding also results in the recruitment of targets to transcriptionally active chromatin subdomains enriched in methylated H3-Lys4 and RNA polymerase II, and thereby prevents the seclusion of targets in

nuclear subdomains where chromatin is more compacted and rich in methylated H3-Lys27 (**Figure 7**).

Previous studies have shown that genes are preferentially transcribed in nuclear subdomains enriched in RNA polymerase II (Grande et al., 1997;Iborra et al., 1996;Osborne et al., 2004;Ragoczy et al., 2006). This has led to models postulating that active loci loop into regions with high local RNA polymerase II concentrations (Cook, 2002;Osborne et al., 2004;Ragoczy et al., 2006). Our findings provide strong confirmation that gene activity is associated with RNA polymerase II domains in primary cells, and represent a genetic demonstration that this is an activator-dependent process. Importantly, it extends our understanding of this phenomenon by showing it entails the relocation of genes among compartments that differ in the composition of histone modifications known to be critically involved in transcriptional regulation (Cao et al., 2002;Plath et al., 2003;Santos-Rosa et al., 2002;Schubeler et al., 2004;Strahl et al., 1999).

These findings can be related to the association of gene silencing with peripheral positioning (Gasser, 2001;Kosak et al., 2002;Kosak and Groudine, 2004;Zink et al., 2004), inasmuch as H3-Lys27me3-rich regions exhibit a more peripheral and perinucleolar distribution than RNA polymerase II foci (**Fig.2G, Fig.4C,D, Fig.5C,D, Supplementary Fig1M,P.** and **Supplementary video3**). Paradoxically, inducible gene activation in yeast has also been linked to the relocation to peripherally located nuclear pore complexes (Casolari et al., 2004), suggesting that radial distances represent a surrogate measure of functional subdomains. It is thus conceivable that the peripheral location of silenced genes

specifically correlates with repositioning to H3-Lys27me-rich/ RNA polymerase II-poor domains.

The concordance between local and subnuclear histone modification patterns in Hnf1α-dependent loci suggests that activator-induced local histone modifications and spatial locus repositioning could be mechanistically linked. Chromosomal loci have been shown to be highly mobile within the nucleus, and different individual loci appear to exhibit different motile properties (Chubb and Bickmore, 2003;Heun et al., 2001). On the other hand, it has been shown that histone modifications such as acetylation can increase chromatin fiber flexibility (Krajewski and Becker, 1998). It is thus likely that local activator-dependent histone modifications and chromatin remodeling result in increased mobility and loop formation, thus providing an increased likelihood of accessing RNA polymerase II-rich foci. Increased access may result in compartmentalization of active loci, if dynamic contacts are stabilized by high-affinity interactions between locus-bound activation complexes and RNA polymerase II, or by the transcriptional process per se (Cook, 2002). In contrast, activator deficiency is expected to result in a more restricted chromatin motion, resulting in target loci remaining partitioned to more condensed chromatin domains devoid of RNA polymerase II.

Emerging evidence indicates that the transcription of the genome is an integrated multi-level regulatory process (Kosak and Groudine, 2004;van Driel et al., 2003).The data presented here links the function of an activator at different levels, namely the binding to specific target sequences, the local modification of target chromatin, and the repositioning of targets in nuclear domains. This is demonstrated in a genetic model of human diabetes, indicating

that nuclear delocalization of chromosomal loci forms part of the cellular defect of a human transcriptional disease. These findings thus provide insights into the mechanisms underlying both gene transcription and disease.

Material and Methods

Cell preparation. Hepatocytes and islets were isolated from 4-6-week-old *Hnf1*$\alpha^{+/+}$ and *Hnf1*$\alpha^{-/-}$ mice (Lee et al., 1998) as described (Boj et al., 2001;Parrizas et al., 2001). Islets were then gently dissociated for 2 min in pre-warmed trypsin solution.

RNA extraction and RT-PCR. RNA isolation, reverse transcription and PCR were as described (Boj et al., 2001).

General DNAse I sensitive assay. Isolated hepatocytes (30-40.10^6) were resuspended in 10 mL NI buffer (15 mM Tris-HCl pH7.5, 300 mM sucrose, 15 mM NaCl, 60 mM KCl, 4 mM MgCl2 and 0.5 mM DTT), and 10 mL of NI buffer supplemented with 1% NP40 was added for 10 min incubation in ice. Nuclei were collected at 500xg for 3 min, washed in 4 mL NI buffer, resuspended in a final volume of 700 μL NI buffer and distributed in 100 μL aliquots for DNAse I digestion. To each suspension of 100 μL NI buffer, either 0, 10, 20, 30, 40, 50 or 80 μg DNAse I was added for 10 min on ice. The reaction was stopped with Nuclei Lysis Solution from Wizard Genomic DNA purification kit (Promega), and DNA was extracted as indicated by the manufacturer. DNAs were resuspended in 20 μL DNA rehydration solution and 1 μL was used for PCR amplification. Oligonucleotides specific for the transcription start site and coding sequences of the *Cyp2j5* and *Actb* genes are presented in **Supplementary Table 1**.

Chromatin Immunoprecipitation. Approximately 2.10^6 isolated hepatocytes were used per immunoprecipitation as described (Mellitzer et al., 2006;Parrizas et al., 2001), with modifications. Immunoprecipitations were carried out overnight at 4ºC with 7.5 µg rabbit anti-HNF1 (H-205) (Santa Cruz, sc8986), 2 µg rabbit anti-H3-Lys4me2 (Upstate, 07-030), 2 µg mouse anti-H3-Lys27me2,3 (Sarma et al., 2004) (D. Reinberg, University of Medicine and Dentistry of New Jersey), 10 µg rabbit anti-H3-Lys27me3 (Peters et al., 2003) (T. Jenuwein, The Vienna Biocenter and Upstate, 07-449) or 20 µg rabbit anti-H3-Lys9me3 (Peters et al., 2003) (T. Jenuwein and Upstate, 07-442). For anti-H3-Lys4me2 and H3-Lys27me2,3, 1% Triton was added to the antibody binding solution. For anti-H3-Lys27me2,3, 3 µg rabbit anti-mouse IgG (Sigma) was added for a further 3 hr incubation at 4ºC. Immune complexes were collected by adsorption to protein A+G Sepharose (Amerhsam). Beads were washed and eluted as described, except for the anti-H3-Lys9me3 immunoprecipitation that was washed with 250 mM NaCl. Purified immunoprecipitated DNA was analyzed in duplicate by SYBR green real-time PCR, and compared to a standard curve generated with serial dilutions of input chromatin DNA. Oligonucleotides are shown in **Supplementary Table 1.**

Immunofluorescence. 50.000 isolated hepatocytes or islet-cells were lightly cytospun and fixed at room temperature for 15 min in freshly prepared 4% paraformaldehyde, washed in PBS, and heated in a microwave in 10 mM citrate buffer, pH 6 for 5 min. In control experiments, fixation was carried out in methanol at -20ºC for 10 min. Immunostaining was carried out as described (Maestro et al., 2003), using primary antibodies with the following dilutions:

rabbit anti-H3 (Abcam, Ab1791) (1/500), rabbit anti H3-Lys4me2 (Upstate, 07-030) (1/500), rabbit anti H3-Lys9me3 (Peters et al., 2003) (T. Jenuwein, The Vienna Biocenter and Upstate, 07-442) (1/500), mouse anti-H3-Lys27me3 (Abcam, Ab 6002) (1/50), rabbit anti H3-Lys27me3 (Peters et al., 2003) (T. Jenuwein and Upstate, 07-449) (1/500), rabbit anti H3-Lys27me2 (Peters et al., 2003) (T. Jenuwein, The Vienna Biocenter) (1/500), rabbit anti H3-Lys27me1 (Upstate, 07-448) (1/500), mouse anti-RNA polymerase II CTD4H8 (Abcam, Ab 5408) (1/1000), mouse anti-HNF1α (Transduction Laboratories, H69220) (1/50), and rabbit anti-HNF1 (H-205) (Santa Cruz, sc8986) (1/100). The specificity of methylated H3-Lys27 stainings was verified by co-staining with two different highly specific antibodies directed against the same epitope. The specificity of anti-HNF1α staining patterns was verified by using two different antibodies, by using *Hnf1*$\alpha^{-/-}$ cells, and with alternate fixation procedures (**Fig. 3 and Supplementary Fig.2**). Secondary antibodies were donkey anti-mouse Cy2 and donkey anti-rabbit Cy3 (Jackson ImmunoResearch), both used at 1/200. Nuclear DNA was counterstained with DAPI (1/50,000).

DNA Immuno-FISH. We used purified BAC DNA (**Supplementary Table 2**) for labeling with Dig-nick translation or BioNick kits (Roche). Immuno-FISH was based on modifications of the protocol described by Brown et al (Brown et al., 1997). Cells were immunostained as described above, post-fixed in 4% paraformaldehyde for 15 min, denatured in NaOH 0.1M in PBS, pH 13 for 110 sec, and then washed in cold PBS and 2x SSC. One μL digoxigenin-labeled probe in 14 μL hybridization buffer (50% formamide, 2x SSC, 125 μg/mL Cot-1 and 10% dextran sulphate) and 1 μg mouse Cot-1 (Invitrogen) were denatured

for 5 min at 90ºC. Probes were hybridized overnight at 37ºC, and sequentially washed in 2x SSC, 1x SSC, PBS-triton 0.2% and PBS for 5 min at room temp. Slides were then sequentially incubated with Sheep anti-digoxigenin antibody (Roche) (1/300) for 3 h, and donkey anti-sheep Cy3 antibody (Jackson Immunoresearch) (1/200) for 2 h at room temp., with washes after each step. Cells were mounted with ProLong Antifade (Amersham).

Two-color DNA FISH. Cells were fixed in 4% paraformaldehyde for 15 min at room temperature, washed in PBS and permeabilized for 30 min in PBS-0.5% Triton X-100. Cells were then heated in 10 mM citrate buffer, pH 6 for 5 min and post-fixed in 4% paraformaldehyde. After washing in PBS, cells were incubated in 2x SSC. One μL digoxigenin-labeled probe and one μL biotin-labeled probe were added to 14 μL hybridization buffer (50% formamide, 2x SSC, 125 μg/mL Cot-1 and 10% dextran sulphate) supplemented with 1 μg mouse Cot-1 (Invitrogen). Both probes and cells were simultaneously heated at 90ºc for 5 min to denature DNA, and hybridized and washed essentially as in the immuno-FISH protocol. The digoxigenin-labeled probe was detected with sheep anti-digoxigenin antibody as in the immuno-FISH procedure, and the biotin-labeled probe was detected with AF488-streptavidin (Molecular Probes)(1/500). Cells were washed and counterstained with Topro (Molecular Probes)(1/50,000) and mounted with ProLong Antifade (Amersham).

Image collection. Confocal images for each fluorochrome were acquired sequentially at room temperature with a Leica TCS SL laser scanning confocal spectral microscope, using a 63x oil immersion objective lens (NA 1.32). The

pinhole was set at 1 Airy unit, giving an axial resolution of 475 nm, and zoom (x4) was used for maximum image resolution (image pixel size 58nm). Focal Check Fluorescent microspheres (Molecular Probes) were used to align laser lines. Non-saturated, unprocessed images were further analyzed with ImageJ. Contrast-stretch and gamma adjustments were made using Photoshop (Adobe) only for display. Processing for colocalization analysis is described below.

Colocalization analysis of covalent histone modifications and RNA Polymerase II. The purpose of this analysis was to determine to what extent there is colocalization of the most intense signals of each epitope. Ten to twenty nuclei were assessed in each double immunofluorescence experiment, and pixels with values exceeding the 75th percentile in each channel were selected for further analysis. The rationale for this threshold is that nuclear RNA polymerase II and H3-Lys27me3 signal intensities do not adhere to a normal distribution, and the 75th percentile enabled separation of visually evident RNA polymerase II and H3-Lys27me3-enriched domains from most remaining nuclear signals. Signals filtered in this manner were used to calculate Manders' coefficient of colocalization using the appropriate ImageJ plug-in (Wayne Rasband and Tony Collins, www.uhnresearch.ca/wcif). Manders' coefficient calculates, for each channel, the proportion of colocalizing pixels respect to the summed up intensities of all pixels in the nucleus. Comparable results were obtained by subtracting pixels lower than the 50th percentile in each channel, and then applying a modified Mander's coefficient using the Colocalization threshold ImageJ plug-in, that first calculates an automated threshold (% colocalized pixels above threshold: RNA polymerase II vs. H3-Lys9me3: 4%.

RNA polymerase II vs. H3-Lys27me3: 19%. RNA polymerase II vs. H3-Lys4me2: 73%. H3-Lys27me3 vs. H3-Lys4me2: 22.5%. H3-Lys27me3 vs. H3-Lys9me3: 31%).

Immuno-FISH image analysis. For each condition, typically 100 alleles (range 70-200) from at least two independent experiments were analyzed blindly in unprocessed images to quantify signal intensities of histone marks and RNA polymerase II. In H3-Lys27me3 experiments Barr bodies were avoided. The 9-pixel area containing the brightest and most central pixels of each FISH signal was selected by inspection of single color images, and the average signal for each channel in this area was obtained using RGB Measure (ImageJ). Each non-thresholded immunofluorescence signal at a FISH-detected locus was divided by the median value of the entire nucleus in the same cell to correct for cell to cell and inter-assay technical variability (legended as *normalized signal* in Figures 4-5). The mean intensity for each channel was also calculated from a broad cytoplasmic area in every stack and used to subtract non-specific background from both FISH and nuclear signals. This value was similar to the non-specific nuclear signal elicited in control Immuno-FISH experiments in which primary antibodies were omitted.

To classify alleles according to the presence or absence of enrichment in either RNA polymerase II or a histone mark, we used the 75th percentile of nuclear pixel intensities in each channel as the threshold, as described above. The results presented here remained statistically significant with alternate thresholds to define enrichment, such as the nuclear median (data not shown).

Two-color DNA FISH image analysis. Approximately 100 alleles were analyzed blindly in unprocessed images to quantify the distance between the center of two FISH signals defined by the 9-pixel square area containing the brightest and most central pixels, essentially as described for immuno-FISH analysis. Two alleles were scored as colocalizing if the distance separating two FISH signals were separated by less than 4.24 pixels (0.25 μm), which corresponds to the calculated maximal distance allowed for two contacting 9-pixel areas.

Statistical analysis. Unpaired two-tailed Student's *t*-test was performed for comparison of ChIP, quantitative immuno-FISH studies and allele distances. Chi-square was used for comparison of qualitative immuno-FISH and dual-color FISH results. ANOVA was used for comparison of dual immunofluorescence average colocalization coefficients.

Acknowledgements:

We thank Natalia del Pozo for breeding mice, Frank Gonzalez (NCI) for *Hnf1*$\alpha^{-/-}$ mice, Karen Brown for sharing advice on published protocols, Inma Hernandez-Muñoz, Sylvia F. Boj, Joan M. Servitja, and Carine Nicot for critical reading and valuable discussions, Thomas Jenuwein and Danny Reinberg for antisera, Carina Cardalda for scoring alleles, Francesc Climent for support, and the Confocal microscopy unit of the University of Barcelona School of Medicine.

Author contributions:

RFL, MAM, and JF conceived and designed the experiments. RFL and MAM performed the experiments. RFL, MAM, and JF analyzed the data. RFL and JF wrote the paper.

Funding:

This work was funded by the Ministerio de Educación y Ciencia (SAF2005-00850) and a VI Framework Integrated Project of the European Commission (Betacelltherapy). RFL is a recipient of PhD studentship from the Generalitat de Catalunya (AGAUR).

Abbreviations:

3D, three dimensional; Afm, afamin; Cyp2j5, cytochrome P450, family 2, subfamily j, polypeptide 5; H3-Lys4me2, Histone 3 dimethyl lysine 4; HNF1α, Hepatocyte nuclear factor 1α; Kif12, kinesin factor 12; MODY, Maturity-Onset diabetes of the young; Pah, phenylalanine hydroxilase; RNA Pol II, RNA polymerase II;.Tbp, TATA-binding protein.

References:

Boj, S.F., M.Parrizas, M.A.Maestro, and J.Ferrer. 2001. A transcription factor regulatory circuit in differentiated pancreatic cells. *Proc Natl Acad Sci USA* 98:14481-14486.

Bolzer, A., G.Kreth, I.Solovei, D.Koehler, K.Saracoglu, C.Fauth, S.Muller, R.Eils, C.Cremer, M.R.Speicher, and T.Cremer. 2005. Three-dimensional maps of all chromosomes in human male fibroblast nuclei and prometaphase rosettes. *Plos Biol* 3:826-842.

Branco, M.R. and A.Pombo. 2006. Intermingling of chromosome territories in interphase suggests role in translocations and transcription-dependent associations. *Plos Biol* 4:780-788.

Brown, K.E., S.Amoils, J.M.Horn, V.J.Buckle, D.R.Higgs, M.Merkenschlager, and A.G.Fisher. 2001. Expression of alpha- and beta-globin genes occurs within different nuclear domains in haemopoietic cells. *Nature Cell Biol* 3:602-606.

Brown, K.E., J.Baxter, D.Graf, M.Merkenschlager, and A.G.Fisher. 1999. Dynamic repositioning of genes in the nucleus of lymphocytes preparing for cell division. *Mol Cell* 3:207-217.

Brown, K.E., S.S.Guest, S.T.Smale, K.Hahm, M.Merkenschlager, and A.G.Fisher. 1997. Association of transcriptionally silent genes with Ikaros complexes at centromeric heterochromatin. *Cell* 91:845-854.

Cao, R., L.J.Wang, H.B.Wang, L.Xia, H.Erdjument-Bromage, P.Tempst, R.S.Jones, and Y.Zhang. 2002. Role of histone H3 lysine 27 methylation in polycomb-group silencing. *Science* 298:1039-1043.

Casolari, J.M., C.R.Brown, S.Komili, J.West, H.Hieronymus, and P.A.Silver. 2004. Genome-wide localization of the nuclear transport machinery couples transcriptional status and nuclear organization. *Cell* 117:427-439.

Chakalova, L., E.Debrand, J.A.Mitchell, C.S.Osborne, and P.Fraser. 2005. Replication and transcription: Shaping the landscape of the genome. *Nature Rev Genet* 6:669-677.

Chambeyron, S. and W.A.Bickmore. 2004. Chromatin decondensation and nuclear reorganization of the HoxB locus upon induction of transcription. *Genes Dev* 18:1119-1130.

Chubb, J.R. and W.A.Bickmore. 2003. Considering nuclear compartmentalization in the light of nuclear dynamics. *Cell* 112:403-406.

Cobb, B.S., S.Morales-Alcelay, G.Kleiger, K.E.Brown, A.G.Fisher, and S.T.Smale. 2000. Targeting of Ikaros to pericentromeric heterochromatin by direct DNA binding. *Genes Dev.* 14:2146-2160.

Cook, P.R. 2002. Predicting three-dimensional genome structure from transcriptional activity. *Nature Genet* 32:347-352.

Cremer, T. and C.Cremer. 2001. Chromosome territories, nuclear architecture and gene regulation in mammalian cells. *Nature Rev Genet* 2:292-301.

Dernburg, A.F., K.W.Broman, J.C.Fung, W.F.Marshall, J.Philips, D.A.Agard, and J.W.Sedat. 1996. Perturbation of nuclear architecture by long-distance chromosome interactions. *Cell* 85:745-759.

Felsenfeld, G. and M.Groudine. 2003. Controlling the double helix. *Nature* 421:448-453.

Ferrer, J. 2002. A genetic switch in pancreatic beta-cells - Implications for differentiation and haploinsufficiency. *Diabetes* 51:2355-2362.

Francastel, C., W.Magis, and M.Groudine. 2001. Nuclear relocation of a transactivator subunit precedes target gene activation. *Proc Natl Acad Sci USA* 98:12120-12125.

Gasser, S.M. 2001. Positions of potential: Nuclear organization and gene expression. *Cell* 104:639-642.

Gilbert, N., S.Boyle, H.Fiegler, K.Woodfine, N.P.Carter, and W.A.Bickmore. 2004. Chromatin architecture of the human genome: Gene-rich domains are enriched in open chromatin fibers. *Cell* 118:555-566.

Grande, M.A., d.K.van, I, L.de Jong, and R.van Driel. 1997. Nuclear distribution of transcription factors in relation to sites of transcription and RNA polymerase II. *J. Cell Sci.* 110 (Pt 15):1781-1791.

Heun, P., T.Laroche, K.Shimada, P.Furrer, and S.M.Gasser. 2001. Chromosome dynamics in the yeast interphase nucleus. *Science* 294:2181-2186.

Iborra, F.J., A.Pombo, D.A.Jackson, and P.R.Cook. 1996. Active RNA polymerases are localized within discrete transcription 'factories' in human nuclei. *J Cell Sci* 109:1427-1436.

Jenuwein, T. and C.D.Allis. 2001. Translating the histone code. *Science* 293:1074-1080.

Kadonaga, J.T. 2004. Regulation of RNA polymerase II transcription by sequence-specific DNA binding factors. *Cell* 116:247-257.

Klymenko, T. and J.Muller. 2004. The histone methyltransferases Trithorax and Ash1 prevent transcriptional silencing by Polycomb group proteins. *EMBO Rep.* 5:373-377.

Kosak, S.T. and M.Groudine. 2004. Form follows function: the genomic organization of cellular differentiation. *Genes Dev* 18:1371-1384.

Kosak, S.T., J.A.Skok, K.L.Medina, R.Riblet, M.M.Le Beau, A.G.Fisher, and H.Singh. 2002. Subnuclear compartmentalization of immunoglobulin loci during lymphocyte development. *Science* 296:158-162.

Krajewski, W.A. and P.B.Becker. 1998. Reconstitution of hyperacetylated, DNase I-sensitive chromatin characterized by high conformational flexibility of nucleosomal DNA. *Proc Natl Acad Sci USA* 95:1540-1545.

Lee, Y.H., B.Sauer, and F.J.Gonzalez. 1998. Laron dwarfism and non-insulin-dependent diabetes mellitus in the Hnf-1 alpha knockout mouse. *Mol Cell Biol* 18:3059-3068.

Maestro, M.A., S.F.Boj, R.F.Luco, C.E.Pierreux, J.Cabedo, J.M.Servitja, M.S.German, G.G.Rousseau, F.P.Lemaigre, and J.Ferrer. 2003. Hnf6 and Tcf2 (MODY5) are linked in a gene network operating in a precursor cell domain of the embryonic pancreas. *Hum Mol Genet* 12:3307-3314.

Mager, J., N.D.Montgomery, F.P.M.de Villena, and T.Magnuson. 2003. Genome imprinting regulated by the mouse Polycomb group protein Eed. *Nature Genet* 33:502-507.

Martens, J.H.A., R.J.O'Sullivan, U.Braunschweig, S.Opravil, M.Radolf, P.Steinlein, and T.Jenuwein. 2005. The profile of repeat-associated histone lysine methylation states in the mouse epigenome. *EMBO J* 24:800-812.

Mellitzer, G., S.Bonne, R.F.Luco, C.M.Van De, N.Lenne-Samuel, P.Collombat, A.Mansouri, J.Lee, M.Lan, D.Pipeleers, F.C.Nielsen, J.Ferrer, G.Gradwohl, and H.Heimberg. 2006. IA1 is NGN3-dependent and essential for differentiation of the endocrine pancreas. *EMBO J.* 25:1344-1352.

Merkenschlager, M., S.Amoils, E.Roldan, A.Rahemtulla, E.O'Connor, A.G.Fisher, and K.E.Brown. 2004. Centromeric repositioning of coreceptor loci predicts their stable silencing and the CD4/CD8 lineage choice. *J Exp Med* 200:1437-1444.

Osborne, C.S., L.Chakalova, K.E.Brown, D.Carter, A.Horton, E.Debrand, B.Goyenechea, J.A.Mitchell, S.Lopes, W.Reik, and P.Fraser. 2004. Active genes dynamically colocalize to shared sites of ongoing transcription. *Nature Genet* 36:1065-1071.

Parada, L.A., P.G.McQueen, and T.Misteli. 2004. Tissue-specific spatial organization of genomes. *Genome Biol* 5.

Parrizas, M., M.A.Maestro, S.F.Boj, A.Paniagua, R.Casamitjana, R.Gomis, F.Rivera, and J.Ferrer. 2001. Hepatic nuclear factor 1-alpha directs nucleosomal hyperacetylation to its tissue-specific transcriptional targets. *Mol Cell Biol* 21:3234-3243.

Peters, A.H.F.M., S.Kubicek, K.Mechtler, R.J.O'Sullivan, A.A.H.A.Derijck, L.Perez-Burgos, A.Kohimaier, S.Opravil, M.Tachibana, Y.Shinkai,

J.H.A.Martens, and T.Jenuwein. 2003. Partitioning and plasticity of repressive histone methylation states in mammalian chromatin. *Mol Cell* 12:1577-1589.

Plath, K., J.Fang, S.K.Mlynarczyk-Evans, R.Cao, K.A.Worringer, H.B.Wang, C.C.de la Cruz, A.P.Otte, B.Panning, and Y.Zhang. 2003. Role of histone H3 lysine 27 methylation in X inactivation. *Science* 300:131-135.

Pontoglio, M., J.Barra, M.Hadchouel, A.Doyen, C.Kress, J.P.Bach, C.Babinet, and M.Yaniv. 1996. Hepatocyte nuclear factor 1 inactivation results in hepatic dysfunction, phenylketonuria, and renal Fanconi syndrome. *Cell* 84:575-585.

Pontoglio, M., D.M.Faust, A.Doyen, M.Yaniv, and M.C.Weiss. 1997. Hepatocyte nuclear factor 1 alpha gene inactivation impairs chromatin remodeling and demethylation of the phenylalanine hydroxylase gene. *Mol Cell Biol* 17:4948-4956.

Pontoglio, M., S.Sreenan, M.Roe, W.Pugh, D.Ostrega, A.Doyen, A.J.Pick, A.Baldwin, G.Velho, P.Froguel, M.Levisetti, S.Bonner-Weir, G.I.Bell, M.Yaniv, and K.S.Polonsky. 1998. Defective insulin secretion in hepatocyte nuclear factor 1alpha-deficient mice. *J. Clin. Invest* 101:2215-2222.

Ragoczy, T., M.A.Bender, A.Telling, R.Byron, and M.Groudine. 2006. The locus control region is required for association of the murine beta-globin locus with engaged transcription factories during erythroid maturation. *Genes Dev.* 20:1447-1457.

Santos-Rosa, H., R.Schneider, A.J.Bannister, J.Sherriff, B.E.Bernstein, N.C.Emre, S.L.Schreiber, J.Mellor, and T.Kouzarides. 2002. Active genes are tri-methylated at K4 of histone H3. *Nature* 419:407-411.

Sarma, K., K.Nishioka, and D.Reinberg. 2004. Tips in analyzing antibodies directed against specific histone tail modifications. *Methods Enzymol* 376:255-+.

Schubeler, D., D.M.MacAlpine, D.Scalzo, C.Wirbelauer, C.Kooperberg, F.van Leeuwen, D.E.Gottschling, L.P.O'Neill, B.M.Turner, J.Delrow, S.P.Bell, and M.Groudine. 2004. The histone modification pattern of active genes revealed through genome-wide chromatin analysis of a higher eukaryote. *Genes Dev.* 18:1263-1271.

Soutoglou, E., B.Viollet, M.Vaxillaire, M.Yaniv, M.Pontoglio, and I.Talianidis. 2001. Transcription factor-dependent regulation of CBP and P/CAF histone acetyltransferase activity. *EMBO J* 20:1984-1992.

Strahl, B.D., R.Ohba, R.G.Cook, and C.D.Allis. 1999. Methylation of histone H3 at lysine 4 is highly conserved and correlates with transcriptionally active nuclei in Tetrahymena. *Proc. Natl. Acad. Sci. U.S.A* 96:14967-14972.

Su, R.C., K.E.Brown, S.Saaber, A.G.Fisher, M.Merkenschlager, and S.T.Smale. 2004. Dynamic assembly of silent chromatin during thymocyte maturation. *Nature Genet* 36:502-506.

Turner, B.M. 2002. Cellular memory and the histone code. *Cell* 111:285-291.

52. van Driel, R., P.F.Fransz, and P.J.Verschure. 2003. The eukaryotic genome: a system regulated at different hierarchical levels. *J. Cell Sci.* 116:4067-4075.

Verschure, P.J., I.van der Kraan, E.M.M.Manders, and R.van Driel. 1999. Spatial relationship between transcription sites and chromosome territories. *J Cell Biol* 147:13-24.

Wansink, D.G., W.Schul, I.Vanderkraan, B.Vansteensel, R.Vandriel, and L.Dejong. 1993. Fluorescent Labeling of Nascent Rna Reveals Transcription by Rna Polymerase-Ii in Domains Scattered Throughout the Nucleus. *J Cell Biol* 122:283-293.

Wijgerde, M., F.Grosveld, and P.Fraser. 1995. Transcription Complex Stability and Chromatin Dynamics In-Vivo. *Nature* 377:209-213.

Yamagata, K., N.Oda, P.J.Kaisaki, S.Menzel, H.Furuta, M.Vaxillaire, L.Southam, R.D.Cox, G.M.Lathrop, V.V.Boriraj, X.N.Chen, N.J.Cox, Y.Oda, H.Yano, M.M.Lebeau, S.Yamada, H.Nishigori, J.Takeda, S.S.Fajans, A.T.Hattersley, N.Iwasaki, T.Hansen, O.Pedersen, K.S.Polonsky, R.C.Turner, G.Velho, J.C.Chevre, P.Froguel, and G.I.Bell. 1996. Mutations in the hepatocyte nuclear factor-1 alpha gene in maturity-onset diabetes of the young (MODY3). *Nature* 384:455-458.

Zink, D., M.D.Amaral, A.Englmann, S.Lang, L.A.Clarke, C.Rudolph, F.Alt, K.Luther, C.Braz, N.Sadoni, J.Rosenecker, and D.Schindelhauer. 2004.

Transcription-dependent spatial arrangements of CFTR and adjacent genes in human cell nuclei. *J Cell Biol* 166:815-825.

Zinner, R., H.Albiez, J.Walter, A.H.F.M.Peters, T.Cremer, and M.Cremer. 2006. Histone lysine methylation patterns in human cell types are arranged in distinct three-dimensional nuclear zones. *Histochem Cell Biol* 125:3-19.

Figure Legends:

Figure 1. *Hnf1α* targets that are inactive in *Hnf1α*$^{-/-}$ cells exhibit local enrichment of H3-Lys27me3, decreased H3-Lys4me2, and reduced DNAse I sensitivity.

(**A,B**) RNA expression of *Hnf1α* targets (*Afm, Cyp2j5, Pah, Kif12*) and control genes (*Tbp, Actb, Nanog, Ly9, Hnf1β*) in Embryonic Stem Cells (ESC), spleen, *Hnf1α*$^{+/+}$ (+/+) and *Hnf1α* $^{-/-}$ (-/-) liver (**A**) and islets (**B**). (**C**) Chromatin immunoprecipitation (ChIP) analysis of Hnf1α occupancy in *Hnf1α*-dependent genes (*Afm* and *Cyp2j5*) and controls (*Tbp* and *Nanog*) in *Hnf1α*$^{+/+}$ and *Hnf1α*$^{-/-}$ hepatocytes. (**D-K**) ChIP analysis of H3-Lys4me2, Lys9me3, Lys27me3, and Lys27me2,3 in the 5' flanking regions of Hnf1α-targets (*Afm*, *Cyp2j5* and *Pah*) and controls (*Tbp*, *Nanog* and *Ly9*) in *Hnf1α*$^{+/+}$ and *Hnf1α*$^{-/-}$ hepatocytes. (**L**) ChIP analysis of anti-H3-Lys9me3 in *Hnf1α*$^{+/+}$ and $^{-/-}$ hepatocytes with semi-quantitative PCR amplification of minor satellite repeats. Serially diluted input DNA and immunoprecipitated H3-Lys27me3 were amplified in parallel as positive and negative controls, respectively. (**M**) ChIP analysis of H3-Lys4me2 and H3 Lys27me2,3 in the *Cyp2j5* locus in *Hnf1α*$^{+/+}$ and *Hnf1α*$^{-/-}$ hepatocytes. The position of the studied amplicons is indicated with solid horizontal lines, and is numbered relative to the transcription start site, set at 0. Grey boxes correspond to exons and red lines depict computationally predicted high-affinity Hnf1 binding sites. Results are means ± SEM of the percentage of input DNA immunoprecipitated in 3 independent experiments. (**N**) Representative PCR analysis of *Cyp2j5* and *Actb* 5' flanking and coding sequence regions after digestion of *Hnf1α*$^{+/+}$ and $^{-/-}$ nuclei with indicated amounts of DNAse I. *p< 0.05

and **p< 0.01 relative to *Tbp* in **D,F,H,J** and *Hnf1*$\alpha^{+/+}$ hepatocytes in **E,G,I,K,M**. Black bars represent *Hnf1*$\alpha^{+/+}$ and white bars *Hnf1*$\alpha^{-/-}$ hepatocytes.

Figure 2. Methylated histone H3 marks exhibit a non-random subnuclear distribution.

(**A,D,G**) Dual immunofluorescence confocal analysis of domains enriched in H3-Lys4me2 (**A**), H3-Lys9me3 (**D**) and H3-Lys27me3 (**G**) (in red) compared with RNA polymerase II (in green), or (**J**) H3-Lys4me2 (red) compared to H3-Lys27me3 (green) in interphase hepatocyte nuclei. (**B,E,H,K**) Venn diagrams represent the degree of colocalization of intense signals of each epitope. The mean ± SEM percentage of colocalizing pixels of 10-20 nuclei is shown on one side of each circle. In (**C,F,I,L**), colocalizing pixels are shown in white in a merged image.

Figure 3. Subnuclear distribution of Hnf1α in histone code and RNA polymerase II domains.

(**A,D,G**) Dual confocal immunofluorescence analysis of Hnf1α domains (in red) compared to H3-Lys4me2 (**A**), H3-Lys27me3 (**D**) and RNA polymerase II (**G**) (in green) in interphase hepatocyte nuclei. Venn diagrams (**B, E, H**) and colocalizing pixels (**C, F, I**) are depicted as in **Figure 2**.

Figure 4. Hnf1α-dependent *Cyp2j5* activity in hepatocytes correlates with positioning in RNA polymerase II and histone code domains.

(**A-D**) Representative confocal immuno-FISH analysis in *Hnf1*$\alpha^{+/+}$ and *Hnf1*$\alpha^{-/-}$ hepatocytes of the *Cyp2j5* locus (red) with RNA polymerase II (RNA Pol II,

green) and either H3-Lys4me2 (**A,B**) or H3-Lys27me3 (**C,D**) (blue). A dotted line depicts the region containing the studied locus, which is also shown on one side at higher magnification with only the blue or green channels. (**E-N**) Quantitative total analysis of histone marks and RNA polymerase II in *Cyp2j5* (**J-N**) and control (*Ly9,* **E-I**) loci in *Hnf1*$\alpha^{+/+}$ and *Hnf1*$\alpha^{-/-}$ hepatocytes. For each condition, non-thresholded signal intensities for methylated histone marks and RNA polymerase II in 70-200 FISH alleles were divided by the nuclear median intensity in the same channel, and are referred to as *normalized signal* in the graphs. The H3-Lys27me3/RNA polymerase II signal intensity ratio for each allele was also calculated (mK27/Pol II, **I,N**). The graphs depict mean ± SEM values. (**O-T**). Distribution of *Cyp2j5* (**R-T**) and control (*Ly9,* **O-Q**) alleles into 4 categories according to the simultaneous enrichment (+) or non-enrichment (-) of RNA polymerase II (RNA Pol II) and either H3-Lys4me2 (K4me2, **Q-T**), H3-Lys9me3 (K9me3, **O-R**), or H3-Lys27me3 (K27me3, **P-S**) in *Hnf1*$\alpha^{+/+}$ (black bars) and *Hnf1*$\alpha^{-/-}$ (white bars) hepatocytes. Each allele was scored as enriched (+) or non-enriched (-) depending on whether or not the signal intensity exceeded the 75th percentile of nuclear signals. Alternate thresholds such as the nuclear median yielded comparably significant results. Results are expressed as % of alleles for each genotype. *p< 0.05 and **p< 0.01 relative to *Hnf1*$\alpha^{+/+}$ cells.

Figure 5. Hnf1α-dependent *Kif12* activity in islets correlates with positioning in RNA polymerase II and histone code domains.

(**A-D**) Representative confocal immuno-FISH analysis of the *Kif12* locus (red) with RNA polymerase II (RNA Pol II, green) and either H3-Lys4me2 (**A-B**, blue)

or H3-Lys27me3 (**C-D**, blue) in *Hnf1α*$^{+/+}$ and *Hnf1α*$^{-/-}$ islets. See also Figure legend **4A-D.** (**E-L**) Quantitative analysis of H3-Lys27me3, H3-Lys4me2 and RNA polymerase II in Hnf1α-dependent (*Kif12*, **I-L**) and control (*Ly9,* **E-H**) loci in *Hnf1α*$^{+/+}$ and *Hnf1α*$^{-/-}$ islet-cells essentially as in **Figure 4E-N**. The graphs depict mean ± SEM values. (**M-P**). Distribution of Hnf1α-dependent (*Kif12,* **O-P**) and control (*Ly9,* **M-N**) alleles into 4 categories according to the simultaneous enrichment (+) or non-enrichment (-) of RNA polymerase II (RNA Pol II) and either H3-Lys27me3 (K27me3, **M,O**) or H3-Lys4me2 (K4me2, **N,P**) in *Hnf1α*$^{+/+}$ (black bars) and *Hnf1α*$^{-/-}$ (white bars) islets as depicted in **Figure 4O-T**. *p< 0.05 and **p< 0.01 relative to *Hnf1α*$^{+/+}$ cells.

Figure 6. Spatial resolution of Hnf1α-dependent repositioning.
(**A**) Schematic representation of the relative position and distances in Kb separating the *Cyp2j5* BAC clone and two contiguous telomeric BACs, 68H9 and 114C9. (**B-C**) Two-color DNA FISH of 68H9 (in green) and *Cyp2j5* or 114C9 (in red) in *Hnf1α*$^{+/+}$ hepatocytes. A dotted line depicts the region shown on one side at higher magnification.(**D-E**) Distribution of 68H9 (**D**) and 114C9 (**E**) alleles into 4 categories according to the simultaneous enrichment (+) or non-enrichment (-) of RNA polymerase II (RNA Pol II) and H3-Lys27me3 (K27me3) in *Hnf1α*$^{+/+}$ (black bars) and *Hnf1α*$^{-/-}$ (white bars) hepatocytes as in **Figure 4O-T**, showing no differences between the two genotypes. (**F**) Distance in μm separating the FISH signals of clones 68H9 and either *Cyp2j5* or 114C9 in *Hnf1α*$^{+/+}$ and *Hnf1α*$^{-/-}$ hepatocytes. The graphs depict mean ± SEM values. **p<0.01 relative to *Hnf1α*$^{+/+}$ cells.

Figure 7. Summary model. *Hnf1α*$^{-/-}$: In the absence of Hnf1α, target nucleosomes exhibit increased methylated H3-Lys27 (blue lines), and are more likely to be located in nuclear domains with condensed chromatin enriched in methylated H3-Lys27. *Hnf1α*$^{+/+}$: In wild type cells, Hnf1α (red ovals) binding recruits complexes that lead to site-specific histone acetylation, H3-Lys4 methylation (green lines), and chromatin remodeling, while preventing H3-Lys27 methylation. This results in enhanced chromatin mobility, increasing access to transcriptionally active subnuclear regions enriched in RNA polymerase II (green).

Figure 1

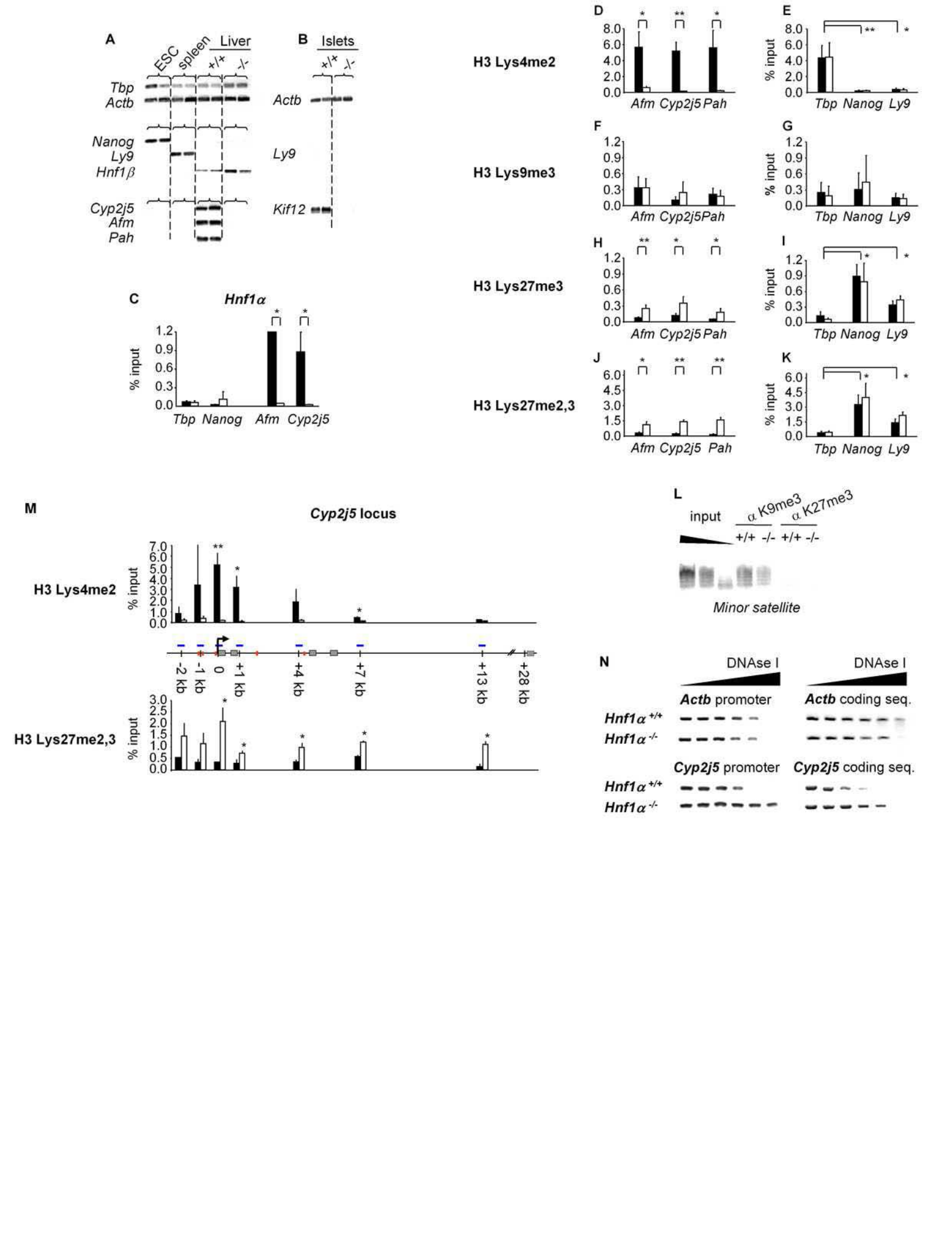
A
ESC
spleen
Liver
+/+
-/-
Tbp
Actb
Nanog
Ly9
Hnf1β
Cyp2j5
Afm
Pah
B
Islets
+/+
-/-
Actb
Ly9
Kif12
C
Hnf1α
% input
Tbp Nanog Afm Cyp2j5
H3 Lys4me2
H3 Lys9me3
H3 Lys27me3
H3 Lys27me2,3
D
E
F
G
H
I
J
K
Afm Cyp2j5 Pah
Tbp Nanog Ly9
M
Cyp2j5 locus
-2 kb
-1 kb
0
+1 kb
+4 kb
+7 kb
+13 kb
+28 kb
L
input
α K9me3
α K27me3
Minor satellite
N
DNAse I
Actb promoter
Actb coding seq.
Cyp2j5 promoter
Cyp2j5 coding seq.
Hnf1α +/+
Hnf1α -/-

Figure 2

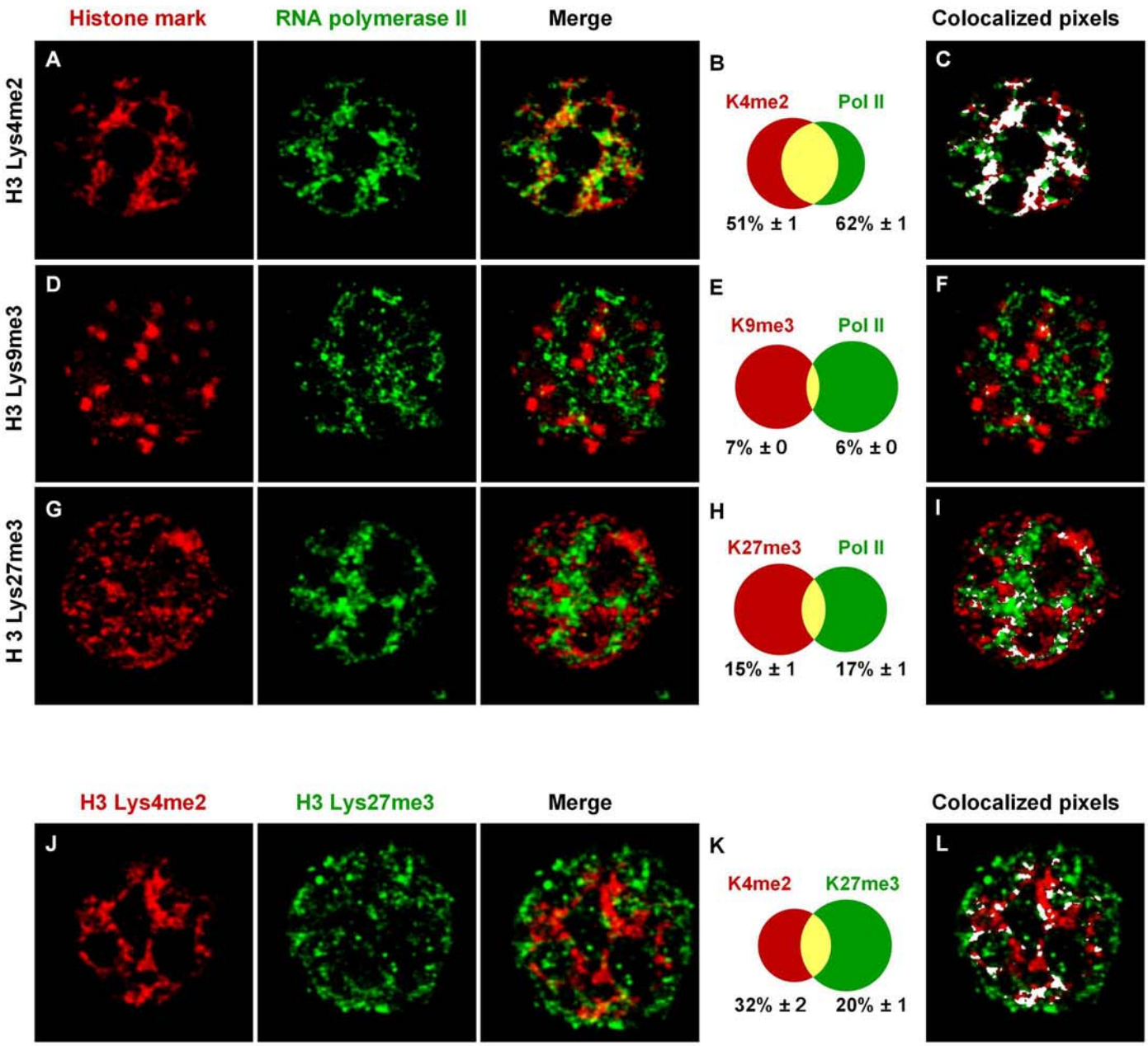
Histone mark
RNA polymerase II
Merge
Colocalized pixels
H3 Lys4me2
H3 Lys9me3
H 3 Lys27me3
A
B
C
D
E
F
G
H
I
K4me2
Pol II
51% ± 1
62% ± 1
K9me3
Pol II
7% ± 0
6% ± 0
K27me3
Pol II
15% ± 1
17% ± 1
H3 Lys4me2
H3 Lys27me3
Merge
Colocalized pixels
J
K
L
K4me2
K27me3
32% ± 2
20% ± 1

Figure 3

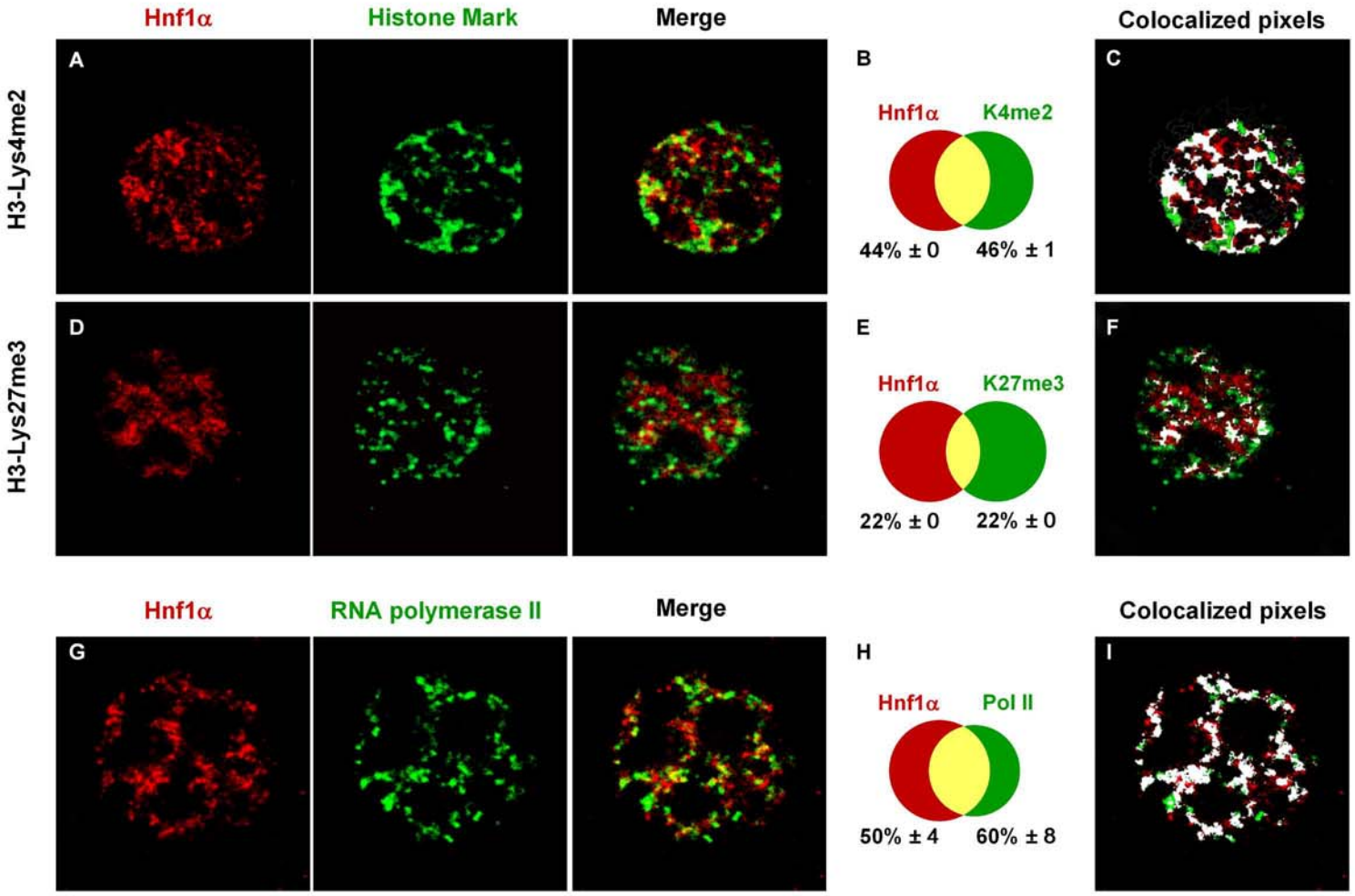
Hnf1α
Histone Mark
Merge
Colocalized pixels
A
B
C
H3-Lys4me2
Hnf1α
K4me2
44% ± 0
46% ± 1
D
E
F
H3-Lys27me3
Hnf1α
K27me3
22% ± 0
22% ± 0
Hnf1α
RNA polymerase II
Merge
Colocalized pixels
G
H
I
Hnf1α
Pol II
50% ± 4
60% ± 8

Figure 4

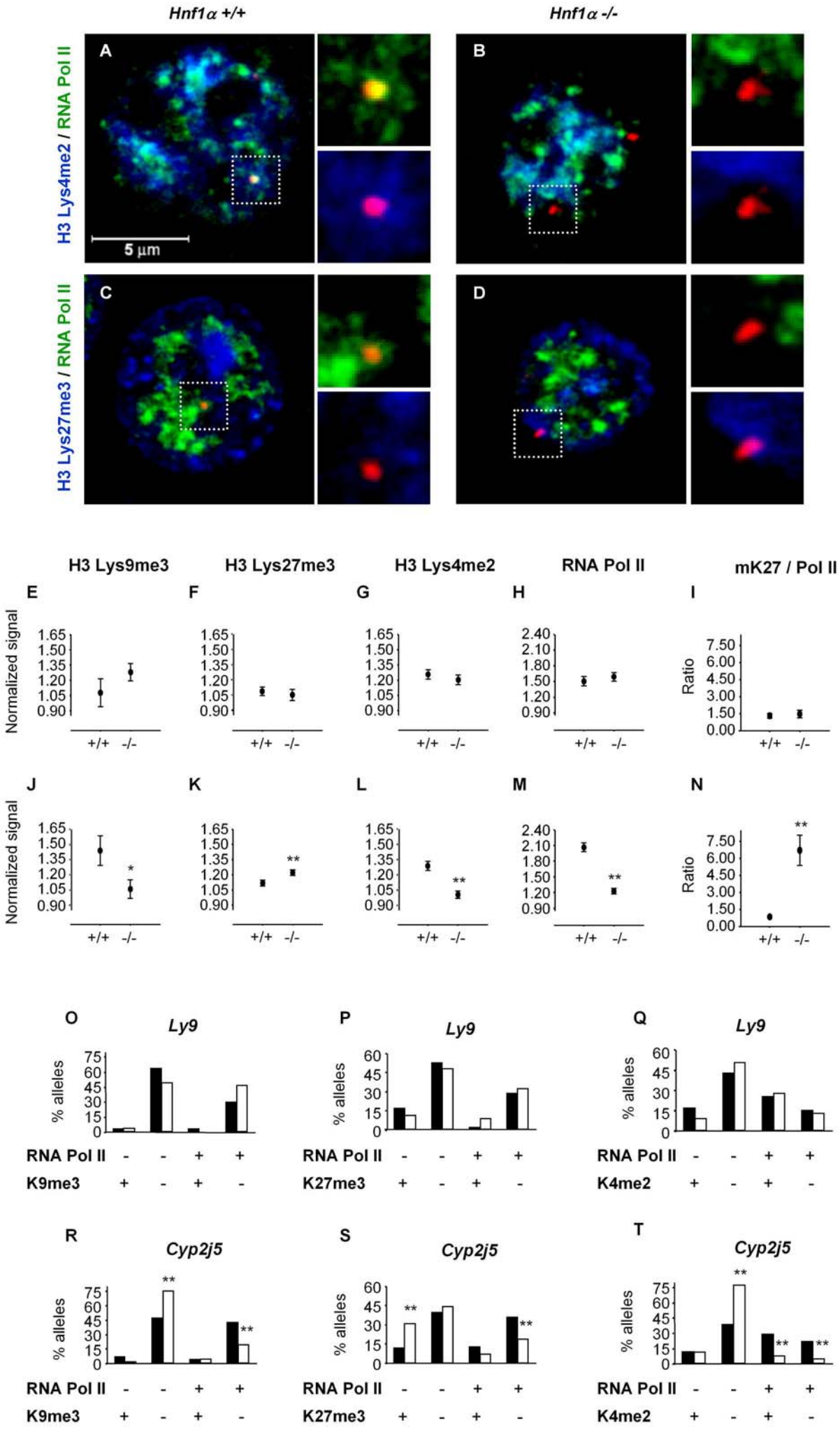
Hnf1α +/+
Hnf1α -/-
H3 Lys4me2 / RNA Pol II
H3 Lys27me3 / RNA Pol II
A
B
C
D
5 μm
H3 Lys9me3
H3 Lys27me3
H3 Lys4me2
RNA Pol II
mK27 / Pol II
E
F
G
H
I
Ly9
Normalized signal
Ratio
+/+
-/-
J
K
L
M
N
Cyp2j5
*
**
O
P
Q
R
S
T
% alleles
RNA Pol II
K9me3
K27me3
K4me2

Figure 5

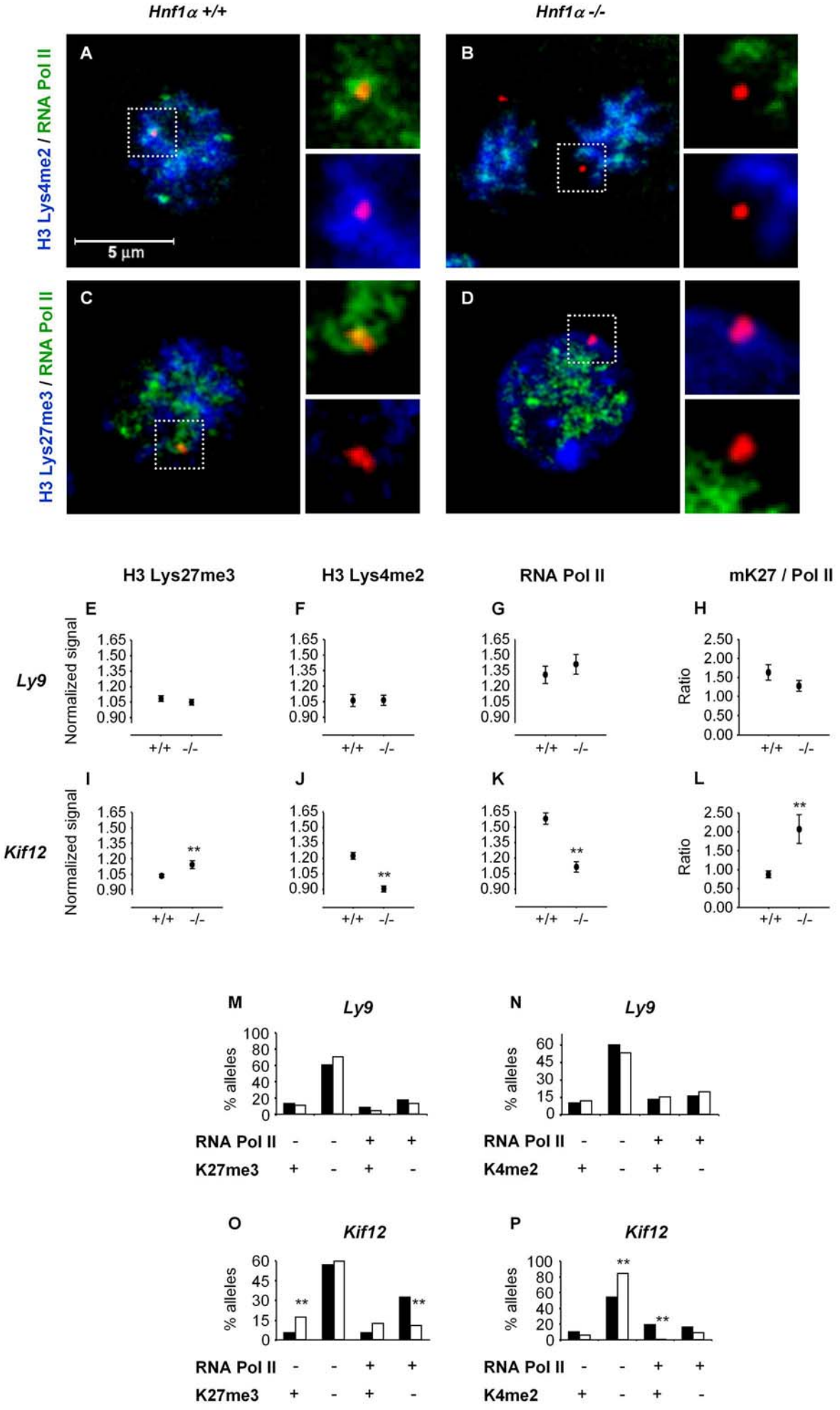
Hnf1α +/+
Hnf1α -/-
A
B
C
D
H3 Lys4me2 / RNA Pol II
H3 Lys27me3 / RNA Pol II
5 µm
H3 Lys27me3
H3 Lys4me2
RNA Pol II
mK27 / Pol II
E
F
G
H
I
J
K
L
Ly9
Kif12
Normalized signal
Ratio
+/+
-/-
**
M
N
O
P
% alleles
RNA Pol II
K27me3
K4me2

Figure 6

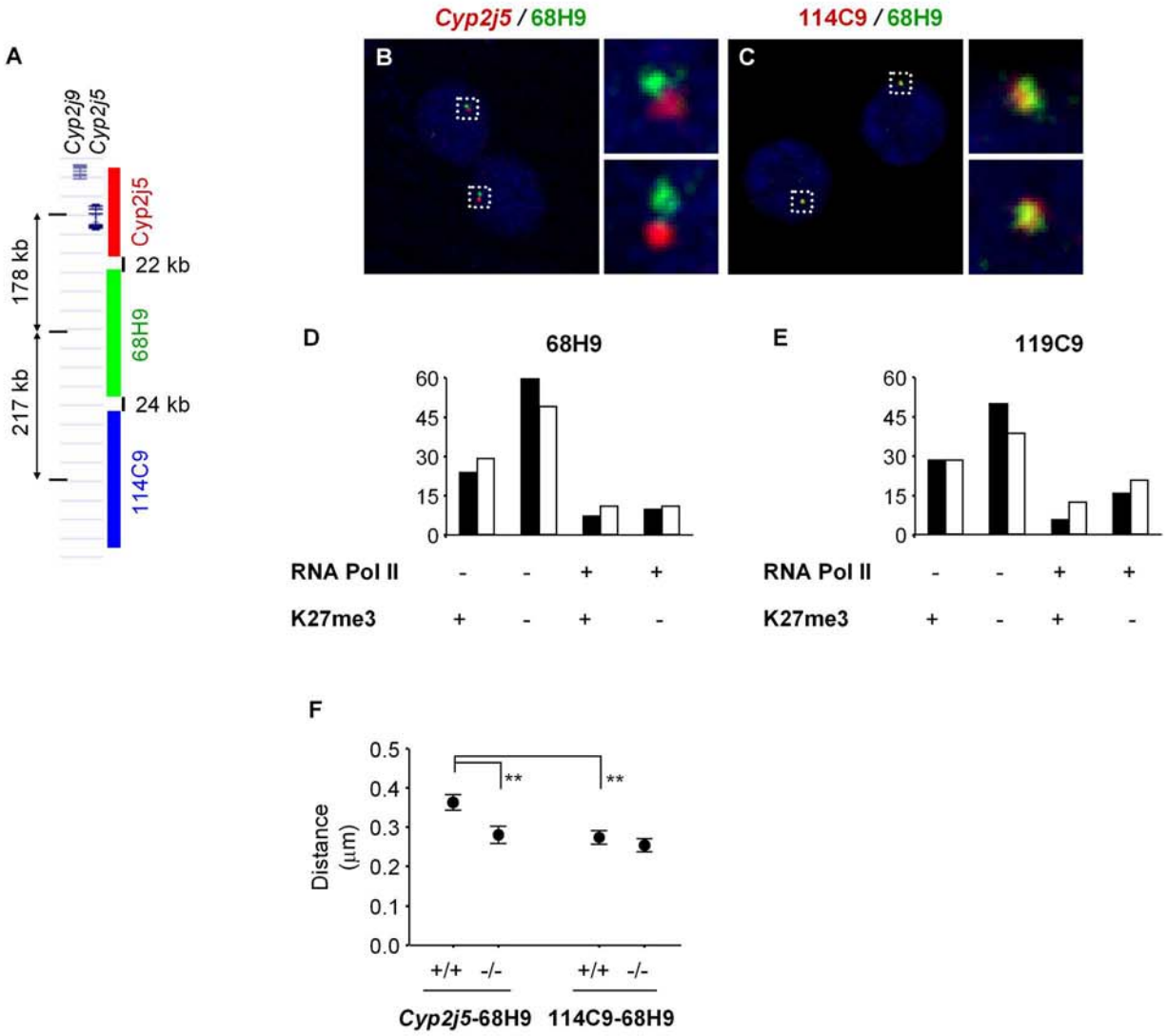
A
Cyp2j9
Cyp2j5
Cyp2j5
22 kb
68H9
24 kb
114C9
178 kb
217 kb
Cyp2j5 / 68H9
114C9 / 68H9
B
C
D
68H9
E
119C9
60
45
30
15
0
RNA Pol II - - + +
K27me3 + - + -
F
Distance (μm)
0.5
0.4
0.3
0.2
0.1
0.0
**
**
+/+ -/-
+/+ -/-
Cyp2j5-68H9
114C9-68H9

Figure 7

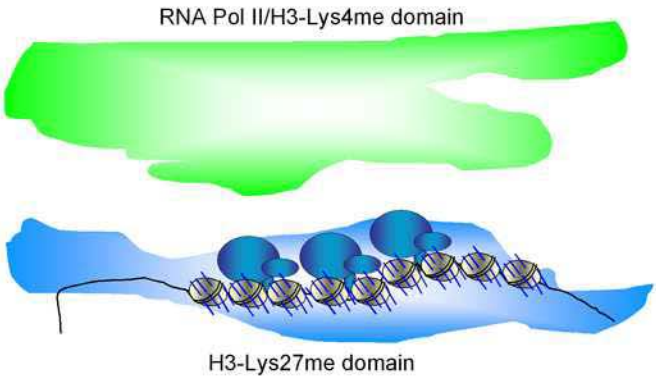

Hnf1α $^{-/-}$

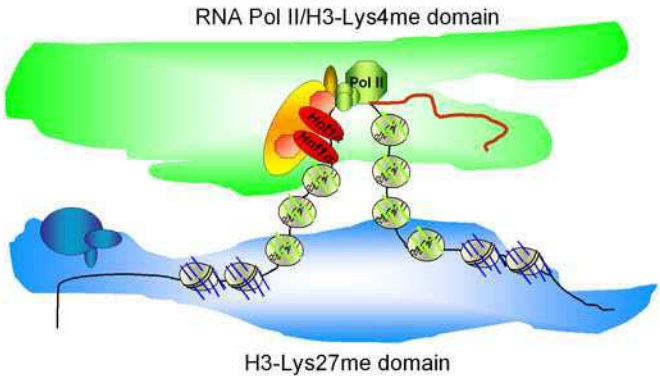

Hnf1α $^{+/+}$

Supplementary Figures legends:

Supplementary Figure 1. (**A-I**) Dual immunofluorescence analysis anti-H3-Lys27me3 (green) and anti-H3-Lys9me2 (**A-C**), anti-H3-Lys9me3 (**D-F**) or anti-H3-Lys27me2 (**G-I**) (red) in hepatocytes. (**J-L**) The H3-Lys27me3 pattern was verified by costaining with a mouse anti H3-Lys27me3 antibody. The use of alternate fixatives, such as methanol (**M-O**), and the FISH procedure (**P-R**) did not alter RNA polymerase II and H3-Lys27me3 nuclear patterns. Manders' coefficients for each channel (**B,E,H,K,N,Q**) and colocalizing pixels in merge images (**C,F,I,L,O,R**) were calculated and described as in **Figure 2**.

Supplementary Figure 2. (**A,D**) Dual immunofluorescence analysis of anti-Hnf1α (in red) and anti-RNA polymerase II (in green) in *Hnf1*$\alpha^{+/+}$ hepatocytes fixed with methanol (**A**) and *Hnf1*$\alpha^{-/-}$ hepatocytes fixed with 4% paraformaldehyde (**D**). Venn diagram (**B**) and colocalizing pixels (**C**) are depicted as in **Figure 2**.

Supplementary Figure 3. Quantitative analysis of H3-Lys27me3 and RNA polymerase II enrichment in control loci (*Hnf1*β, *Actb* and *Nanog*) in *Hnf1*$\alpha^{+/+}$ (+/+) and *Hnf1*$\alpha^{-/-}$ (-/-) hepatocytes as in **Fig 4E-N**. The graphs depict mean ± SEM values. **P< 0.01 relative to *Hnf1*$\alpha^{+/+}$ cells.

Supplementary Figure 4. Immuno-FISH analysis of Hnf1α and RNA polymerase II enrichment in Hnf1α-dependent (*Cyp2j5* and *Afm*) and control loci (*Ly9* and *Actb*) in *Hnf1*$\alpha^{+/+}$ hepatocytes. The graphs depict the percentage of

alleles located in Hnf1α and RNA polymerase II-rich domains. *P<0.05 and **P< 0.01 relative to *Ly9*.

Supplementary videos 1-3. 3D reconstruction of representative confocal dual immunofluorescences in *Hnf1α*$^{+/+}$ hepatocyte nuclei with RNA polymerase II (green) and either H3-Lys4me2 (**1,** blue), H3-Lys9me3 (**2**, blue) or H3-Lys27me3 (**3,** red). About 50-70 frames were collected per nucleus with an 8x magnification. Contrast-stretch, gamma adjustments and 3D reconstruction were done with the Leica TCS SL software and displayed at 20 frames/second.

Supplementary videos 4-5. 3D reconstruction of representative confocal dual immunofluorescences in *Hnf1α*$^{+/+}$ hepatocyte nuclei with (**4**) Hnf1α (red) and RNA polymerase II (green) or (**5**) Hnf1α (green) and H3-Lys27me3 (red), essentially as in videos 1-3.

Gene	Forward	Reverse	Prod. Length (bp)	Annealing (ºC)
Tbp	atcagatgtgcgtcaggcgtt	tgcggagaaaatgacgcga	102	60
Actb (0bp)	gccccgcgtgtccctcaaac	gctccgcgtcgctcactcacc	383	60
Actb coding seq	ggtgtggggagcaggttgg	gtgggtgaagggctagatgtatgg	649	55
Nanog	agaggatgccccctaagcttt	acagttaatcccacctgcagg	103	60
Ly9	gcctgaatccaagaagaggaca	ccagatcctgcaaggaaattgt	140	55
Afm	ctacctgtcaggcaagcacttt	cggtcctggtgcaaatttcta	255	55
Pah	cattgccaggcctgtctgagc	gttgccctgacgtagcagtgga	193	60
Cyp2j5 (0 bp)	gggcaggaaggggtgag	tgacggcttctgaggatgtt	214	60
Cyp2j5 -2Kb	ggctcttacactttcctacaatgg	gccacagaggtcacaaaactattc	155	55
Cyp2j5 -1Kb	tccctcaatgtgagccaatg	ttcatgcctaggacctatgacct	108	55
Cyp2j5 +1Kb	tcgctttatgacaccggttaga	tgttcgaaaccactcacagga	122	55
Cyp2j5 +4Kb	acatctaaggcccacgtaccca	gcaccaccgaggtccaatatt	213	55
Cyp2j5 +7Kb	ggcttctttcacagtgttcctca	ttatgctcagtcttcaactctcgg	137	55
Cyp2j5 +13Kb	tcaacctcacaccagtcagaatg	gaatcccaccaaccatgga	106	55
Cyp2j5 coding seq	tcctctgttttccctcttactcac	tacatgccaccacctctcctac	1296	55

Supplementary Table 1. Oligonucleotide sequences used in chromatin immunoprecipitation analysis

BAC name	Chr. Band	Size (kb)	Gene symbol	Gene name	*Hnf1*$\alpha^{+/+}$ hepatocytes*	*Hnf* hepato
RP23-117I23	6qF1	221.8	*Dppa3*	developmental pluripotency-associated 3	-	
			Nanog	**Nanog**	-	
			Slc2a3	solute carrier family 2	+	
			Foxj2	forkhead box J2	-	
RP23-284L5	5qG2	194.1	*Fbxl18*	F-box and leucine-rich repeat protein 18	-	
			Actb	**actin, beta**	++	+
			Fscn1	fascin homolog 1, actin bundling protein	+	
			Ubce7ip1	ubiquitin conjugating enzyme 7 interacting	-	
RP23-7C5	11qC	235.2	*BC065092*	Riken, hypothetical ARM repeat fold containing	+	N
			Hnf1β	**Hepatocyte nuclear factor 1β**	+	+
			Ddx52	DEAD (Asp-Glu-Ala-Asp) box polypeptide 52	-	
RP23-384B3	1qH3	204.7	*Refbp2*	RNA and export factor binding protein 2	-	
			Itlna	intelectin a	-	
			Cd244	CD244 natural killer cell receptor 2B4	-	
			Ly9	**lymphocyte antigen 9**	-	
			Slamf7	SLAM family member 7	-	
RP24-277J5	4qC5	171.8	*Cyp2j9*	cytochrome P450, family 2, subfamily j	+	**N**
			Cyp2j5	**cytochrome P450, family 2, subfamily j**	++	
RP24-68H9	4qC5	185.6	***68H9***	**No genes**		
RP24-114C9	4qC5-C6	200.9	***114C9***	**No genes**		
RP23-448J19	4qB3 - C1	192.1	***Ambp***	**alpha 1 microglobulin/bikunin**	++	
			Kif12	**kinesin family member 12**	-	
			Col27a1	collagen type XXVII alpha 1	-	
RP24-288B11	5qE1	161.7	***Alb***	**albumin**	++	
			Afm	**afamin**	++	
			Afp	a-fetoprotein	++	+
			RassF6	Ras association domain family 6	+	

Supplementary Table 2. Bacterial artificial chromosomes used in this study * Gene expression is represented as –, + of expression (not expressed, relative low expression, or relative high expression, respectively). ND: not determined. F information has been obtained experimentally by reverse transcription PCR, while for genes marked in black this inform Unigene EST Expression profile viewer (www.ncbi.nlm.nih.gov/entrez). Note that *Hnf1β* mRNA is mildly increased in *H*

Supplemental Figure 1

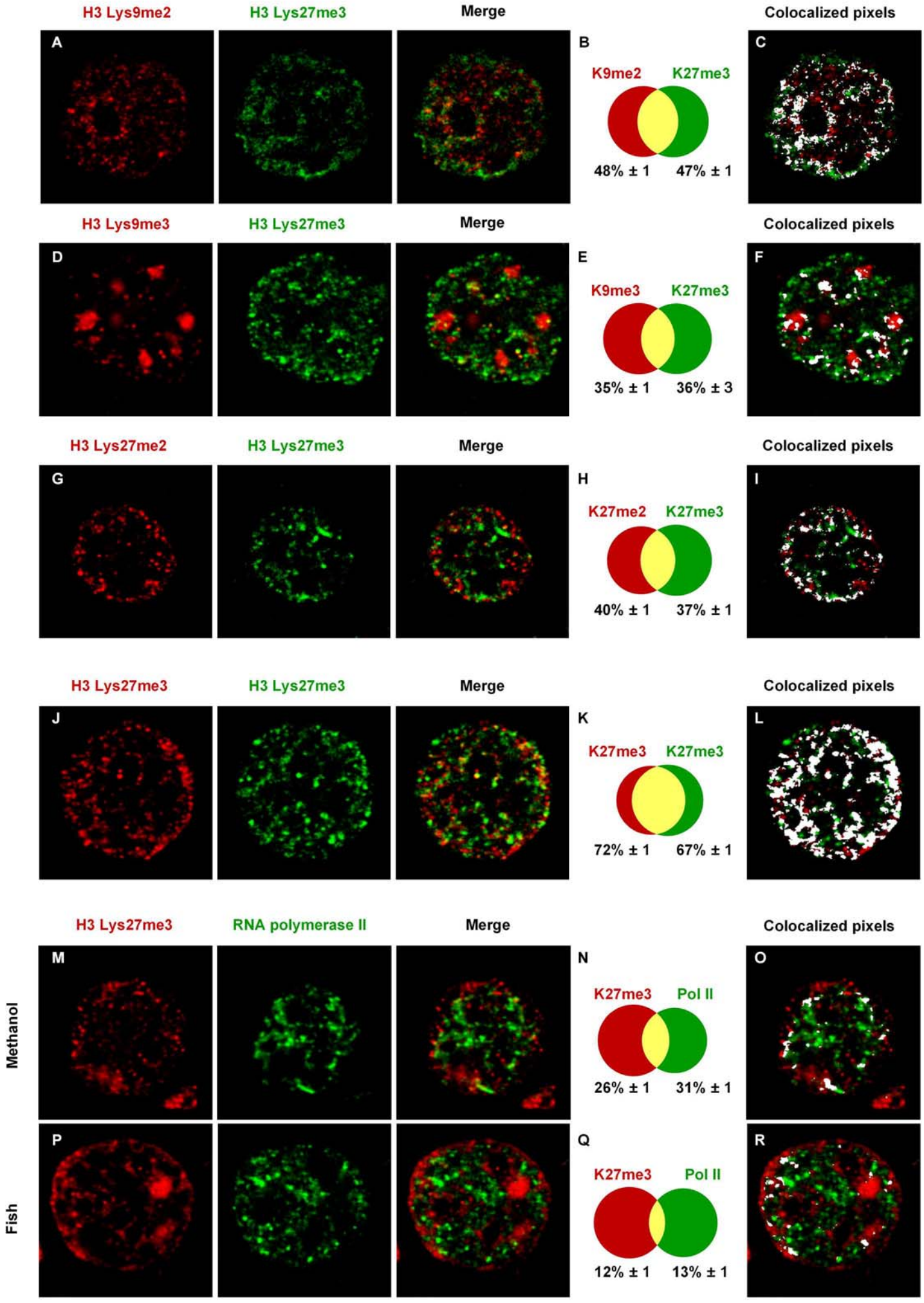

Supplementary Figure 2

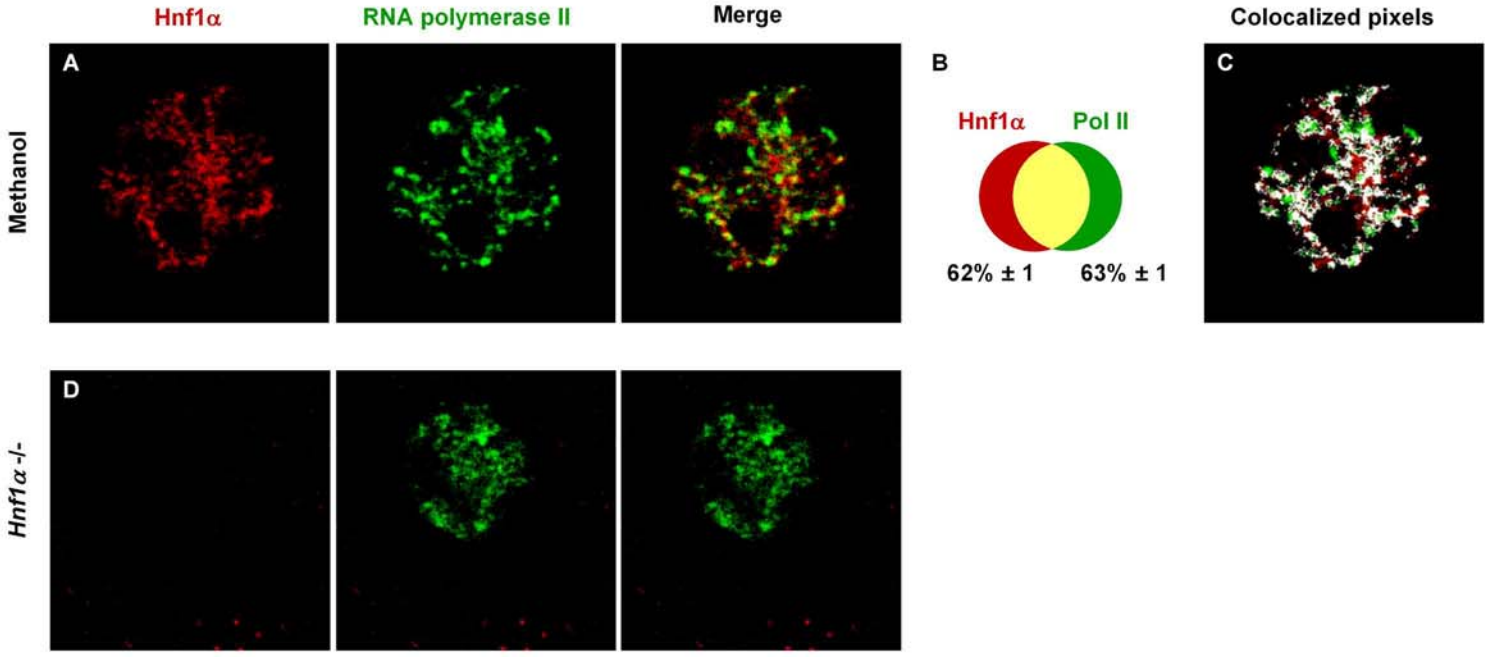

Supplementary Figure 3

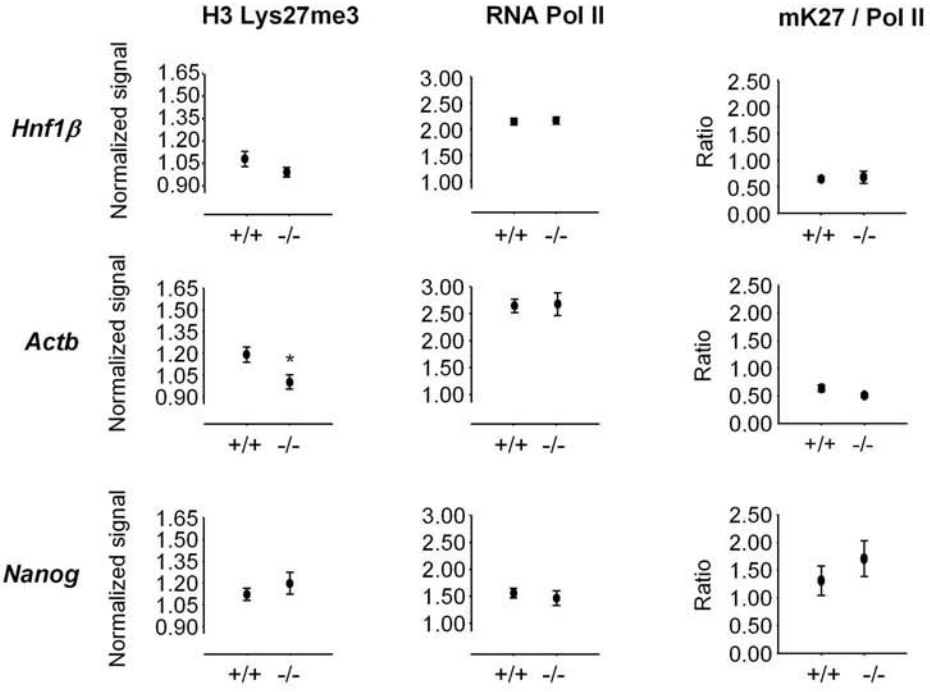

Supplementary Figure 4

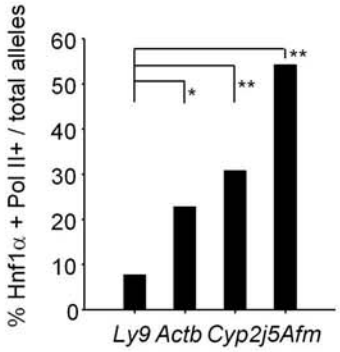

Eliminado: ¶

DISCUSIÓN

Eliminado: ¶

Las mutaciones en el factor de transcripción HNF1α son la causa más frecuente de diabetes tipo MODY. HNF1α se expresa mayoritariamente en células diferenciadas del páncreas, hígado, riñón, e intestino. Se ha visto que HNF1α está implicado en una red transcripcional específica de célula beta, basada en la regulación cruzada de factores de transcripción cuyas mutaciones también causan MODY (PDX1 y HNF4α) (Boj et al., 2001;Shih et al., 2002).

Con este trabajo de tesis hemos intentado comprender la función de HNF1α en un contexto celular. Con un modelo transgénico inducible y tejido-específico, hemos intentado estudiar la autonomía celular de HNF1α en células betas y sus funciones en diferentes momentos del desarrollo.

Por otro lado, basándonos en el modelo deficiente para HNF1α, hemos explorado la relación entre la regulación de la transcripción mediada por un activador a nivel local de las modificaciones de cromatina y a nivel del reposicionamiento génico en el espacio nuclear.

La función de HNF1α en la célula beta tiene autonomía celular

Aparte de expresarse en la célula beta, HNF1α también se expresa en otros tejidos implicados en la regulación de la homeostasis de la glucosa, o bien potencialmente capaces de regular la función de células beta indirectamente, como las células endocrinas del intestino, células pancreáticas no endocrinas, o las células alfa (Thorens and Waeber 1993; Holst 1994; Kieffer and Habener 1999). Sin embargo, al devolver la expresión de HNF1α exclusivamente a la célula beta y no al resto de tejidos, hemos sido capaces de recapitular en parte la función de este activador, sugiriendo que la función de HNF1α en la célula beta parece tener autonomía celular. Esto tiene importancia para el desarrollo de terapias génicas de rescate de función, dirigidas específicamente hacia el tipo celular relevante y así poder reducir posibles efectos secundarios. Sin embargo, debido al fenotipo deletéreo de la sobreexpresión de HNF1α, no hemos podido rescatar el fenotipo diabético, y por lo tanto, no podemos descartar una posible implicación de la función de HNF1α en otros tejidos en la regulación del metabolismo de la glucosa.

La función de HNF1α en la célula beta no parece restringida a las fases iniciales del desarrollo de las células beta.

HNF1α induce la acetilación de histonas y la metilación en H3-Lys4 de sus genes diana. En su ausencia, la cromatina de los genes inactivos está hipoacetilada, metilada en H3-Lys27 y más compacta. La dependencia transcripcional de los genes diana de HNF1α aparece en el momento en que se diferencian las células beta (Boj et al., 2001), lo que plantea la posibilidad que HNF1α remodele la cromatina de sus

genes diana en un momento determinado del desarrollo para establecer una memoria celular. Por otro lado, un estudio previo demostró que la reexpresión *in vitro* de HNF1α en hepatocitos de origen embrionario (E12.2-E13.5) deficiente para HNF1α es capaz de rescatar parcialmente (30% de los niveles normales) la expresión del gen diana *Pah*. Sin embargo, este rescate mediante reexpresión no es posible en hepatocitos adultos deficientes para HNF1α excepto si se emplea una combinación de inhibidores de histona deacetilasas (TSA) y DNA metiltransferasas (5-azaC), cuyo caso se consigue reactivar Pah aunque a niveles muy bajos. Esto sugiere que la función de HNF1α es mantener la cromatina de sus genes diana en conformación abierta, impidiendo que el DNA se metile y que esto debe llevarse a cabo epigenéticamente en el momento adecuado del desarrollo para impedir que los genes diana se heterocromatizen irreversiblemente (Viollet et al., 2001).

Sin embargo, la reinducción postnatal in vivo de HNF1α en islotes deficientes para HNF1α con nuestro sistema inducible y específico de célula beta rescata parcialmente la expresión de diferentes genes diana, como Glut2, sin la ayuda de inhibidores de la heterocromatina. A pesar de la expresión mosaica de nuestro transgén, el nivel de reexpresión de dianas observado en nuestro estudio es en algunos casos de magnitud comparable a la inducción observada en hepatocitos embrionarios en el estudio mencionado previamente, e incluso claramente superior a la observada en hepatocitos adultos. Esto sugiere que el requerimiento de HNF1α en etapas tempranas de la diferenciación es diferente en células beta y hepatocitos.

Las diferencias en la capacidad de HNF1α para remodelar la cromatina y rescatar la expresión de sus genes diana según el tipo celular podrían deberse a diferencias en el patrón de expresión de HNF1α durante el desarrollo. La expresión de HNF1α durante la diferenciación de las células beta debe ser menos crítica que durante la diferenciación de los hepatocitos. Existe un pico de expresión de HNF1α con la maduración de la célula beta, mientras que su parálogo HNF1β se expresa en células precursoras ductales (Maestro et al., 2003)**.** Por el contrario, HNF1α se expresa en hígado desde los inicios del desarrollo. Esto sugiere que HNF1β, que es potencialmente capaz de unirse a las mismas dianas que HNF1α, podría estar supliendo la función de HNF1α durante el desarrollo previo a la formación de las células beta, manteniendo los genes diana en conformación abierta.

Creemos que el rescate incompleto de la función de HNF1α en nuestro modelo podría ser debido a la expresión a niveles no fisiológicos de HNF1α. Sin embargo, no descartamos la necesidad de inhibidores de la heterocromatina (TSA, 5-azaC, RNAi contra Ezh2, por ejemplo) o una reinducción de HNF1α en edad embrionaria para un mejor rescate de la función de HNF1α en célula beta.

HNF1α impide la metilación de H3-Lys27 de sus genes diana.

Estudios genéticos realizados en Drosophila demostraron que el estado por defecto de los genes estudiados es la metilación de H3-Lys27 y la represión vía polycomb, mientras que la presencia de complejos activadores de la familia trithorax no sólo metilan la cromatina en H3-Lys4 sino que también impiden la metilación de H3-Lys27, permitiendo la activación génica. Esto sugiere que la función de estos activadores es inhibir la represión génica. (Klymenko and Muller, 2004). En la segunda parte de este trabajo de tesis, hemos visto que la falta de HNF1α deja a los genes diana inactivos vía la trimetilación de H3-Lys27, pero no se produce una trimetilación de H3-Lys9. También hemos observado una dimetilación de H3-Lys9. En analogía al ejemplo señalado en Drosophila, planteamos que el rol de HNF1α podría ser evitar la represión de sus genes diana mediada por la metilación de H3-Lys27, y ello podría estar ligado a la acetilación y metilación en H3-Lys4 de la cromatina durante la diferenciación de la célula beta. Los genes quedarían en conformación abierta, marcados positivamente y de forma heredable para la transcripción, estableciendo así una memoria celular. En su ausencia, la célula no podría activar toda una serie de genes importantes para la función de la célula beta madura, derivando en diabetes MODY.

En el caso de la célula beta esta función de promover cambios heredables en la cromatina podría estar parcialmente suplida por HNF1β, como se comenta anteriormente, de forma que la simple reaparición de HNF1α permitiría reactivar la transcripción de sus genes diana. No obstante, serán necesarios nuevos modelos para poder comprender en profundidad los factores necesarios para recapitular plenamente la función de HNF1α en edad adulta, de cara al diseño de terapias génicas de rescate de su función en pacientes MODY3.

La función de HNF1α en la célula beta es dependiente de los niveles de expresión.

Otro aspecto importante a la hora de desarrollar terapias génicas o protocolos de diferenciación in vitro de células beta es la cantidad de HNF1α que debe reexpresarse. La sobreexpresión de HNF1α a largo plazo en la célula beta ha demostrado ser más nociva que la pérdida de función. El exceso de HNF1α induce muerte celular, inhibe la proliferación y subsecuentemente reduce la masa de célula beta hasta derivar en diabetes. No creemos que este fenotipo se deba a una ganancia de función, es decir que HNF1α sea un inhibidor de la proliferación, ya que datos no publicados de nuestro laboratorio y de otros laboratorios sugieren que ni la masa de célula beta ni la proliferación de la célula beta están aumentadas en el ratón *Hnf1α*$^{-/-}$ (Pontoglio et al., 1998; RFL, no publicado).

Existen varios mecanismos no exclusivos que pueden explicar el efecto inhibitorio de la sobreexpresión de HNF1α. Por ejemplo, el secuestro de coactivadores que interaccionen con HNF1α, afectando a la expresión de genes esenciales para la célula beta (Parrizas et al., 2001;Soutoglou et al., 2000;Soutoglou et al., 2001b). HNF1α debe heterotetramerizar con DCOH para poderse unir al DNA en el núcleo, sin embargo DCOH es una proteína bifuncional con actividad nuclear y citoplasmática (Hauer et al., 1993). Inmunotinciones en islotes que sobreexpresan HNF1α evidencian una relocalización de DCOH hacia el núcleo, afectando posiblemente a su función citoplasmática como regenerador de la tetrahidrobiopterina (datos no mostrados). Por otro lado, un exceso de síntesis de la proteína HNF1α puede inducir estrés de retículo endoplasmático y apoptosis, con la consecuente reducción de la masa de célula beta (Araki et al., 2003;Cardozo et al., 2005;Kutlu et al., 2003). Sin embargo, existen varios modelos transgénicos dirigidos por el promotor de insulina que no presentan anormalidades, como el propio $Tg^{RIP\text{-}tTA}$, los ratones que expresan la recombinasa Cre o diferentes modelos de rescate de la expresión de proteínas importantes para la célula beta como Glut2, IGF1 o HGF (Bernal-Mizrachi et al., 2001;Garcia-Ocana et al., 2000;George et al., 2002;Grewal et al., 1997;Sund et al., 2001;Thorens et al., 2000;Welsh et al., 1999). Podría ser que los reguladores transcripcionales, en particular, sean especialmente sensibles a variaciones en los niveles de expresión, sobretodo si están implicados en complejas redes transcripcionales, como HNF1α. En la literatura se pueden encontrar diferentes ejemplos de activadores, como AP-2, Ets2 o Pax6, en los que tanto la falta como la sobreexpresión tienen el mismo efecto inhibitorio en la célula (Carbone et al., 2004;Clark et al., 2002;Moser et al., 1997;Wolvetang et al., 2003;Yamaoka et al., 2000;Zhang et al., 2003).

Es interesante señalar que recientemente se ha descrito un fenotipo similar a nuestro modelo doble transgénico pero en líneas celulares y sobreexpresando HNF1β en lugar de HNF1α. La sobreexpresión de HNF1β en la línea celular específica de célula beta Ins-1, inducía apoptosis e inhibía la proliferación y la secreción de insulina en respuesta a metabolitos (Welters et al., 2006). Sorprendentemente, la sobreexpresión de un mutante dominante negativo de HNF1β (A263ins) que sólo conserva la capacidad de dimerizar con HNF1β y HNF1α, no induce ningún fenotipo deletéreo. Sin embargo la sobreexpresión de otra mutación MODY5 (P328del) que conserva cierta capacidad transactivadora, sólo inhibe la proliferación y en menor medida que la versión salvaje. Además la sobreexpresión de HNF1β en otra línea celular (HEK-293) tampoco causaba un fenotipo deletéreo. Recapitulando, parece que las células beta son especialmente sensibles a la sobreexpresión de ciertas proteínas, y en particular a los HNF1 y que la función transactivadora de los HNF1

podría estar implicada en la inhibición de la proliferación pero no en la inducción de apoptosis.

Por último, el análisis confocal de la distribución de HNF1α en el núcleo por inmunofluorescencia reveló que la sobreexpresión de HNF1α altera la colocalización de HNF1α en dominios activos ricos en RNA polimerasa II y H3-Lys4 metilada (datos preliminares). Posiblemente, esta falta de distribución en dominios activos afecte al posicionamiento de los loci dependientes de HNF1α y por lo tanto su actividad transcripcional.

Implicaciones del análisis de la sobreexpresión de un factor de transcripción para la intepretación de estudios basados en la sobreexpresión de factores salvajes y mutantes dominante negativos.

Curiosamente, el fenotipo de pérdida de función obtenido por la sobreexpresión de HNF1α en nuestro transgénico se parece más a los fenotipos descritos por la sobreexpresión de mutaciones dominante negativas de HNF1α que a los modelos deficientes para HNF1α. Los ratones que sobreexpresan versiones mutadas de HNF1α tienen los islotes desestructurados, una pérdida de la masa de célula beta por inhibición del ciclo celular y apoptosis, presentan estrés de retículo endoplasmático y otras anomalías ultraestructurales ausentes en el ratón *Hnf1α*$^{-/-}$ (Hagenfeldt-Johansson et al., 2001;Wobser et al., 2002;Yamagata et al., 2002;Yang et al., 2002;Lee et al., 1998;Parrizas et al., 2001;Pontoglio et al., 1998). La similitud de fenotipos sugiere que al menos parte de la pérdida de función observada en los modelos dominante negativos podría deberse en parte a la sobreexpresión de dominios funcionales de la proteína mutada más que a una pérdida de función (Hagenfeldt-Johansson et al., 2001;Wang et al., 1998;Yamagata et al., 2002).

El hecho que la sobreexpresión de un factor de transcripción pueda tener efectos deletéreos e incluso similares al fenotipo por pérdida de función manifiesta el peligro de usar modelos de sobreexpresión. A menudo se diseñan sistemas de expresión fuertes para devolver la función de un factor de transcripción mediante terapia génica, o para estudiar su rol por ganancia de función. Por otro lado, los protocolos de transdiferenciación y diferenciación artificial de células beta *in vitro* para su posterior transplante suelen basarse en la sobreexpresión de factores de transcripción importantes para el desarrollo de células beta (Blyszczuk et al., 2003;Ferber et al., 2000;Heremans et al., 2002;Miyazaki et al., 2004). Este trabajo apunta a que los factores de transcripción deben expresarse en su justa medida y que tanto la falta como el exceso pueden ser deletéreos para la célula.

El modelo deficiente para HNF1α nos permite estudiar genéticamente en células diferenciadas la función de un activador en el reposicionamiento génico.

Nuestro estudio se basa en un modelo genético *in vivo* deficiente para un activador, de manera que podemos comparar el posicionamiento de un mismo locus según su estado transcripcional en el mismo tipo celular y estado de diferenciación en hepatocitos o islotes de origen primario, a los cuales sólo les falta el factor de transcripción. A pesar de no ser un modelo inducible, es un modelo que asegura cambios directamente asociados a la falta del activador y no a diferencias en el tipo celular. Este aspecto del estudio es importante por dos motivos principales.

En primer lugar, hasta el momento, casi todos los estudios de reposicionamiento génico se han realizado en modelos de desarrollo y líneas celulares transformadas que demuestran un reposicionamiento génico dependiente del estado de diferenciación celular o bien del tipo celular (Brown et al., 2001;Chambeyron and Bickmore, 2004;Zink et al., 2004;Kosak et al., 2002;Merkenschlager et al., 2004;Su et al., 2004;Volpi et al., 2000). Sin embargo, al comparar la posición en diferentes tipos celulares es necesario tener en cuenta que existen diferencias importantes de estructura nuclear y organización genómica según el tipo celular, como por ejemplo el posicionamiento relativo de los territorios cromosómicos en el núcleo (Misteli, 2004).

En segundo lugar, a pesar que se han descrito múltiples ejemplos de reposicionamiento génico en función de la actividad transcripcional (Brown et al., 1997; Cobb, 2000; Gasser, 2001; Chambeyron et al., 2004; Osborne et al., 2004; Kosak et al., 2002; Zink et al.,2004; Merkenschlager, 2004; Su, 2004; Ragozcy et al., 2006), jamás se ha clarificado si el reposicionamiento es debido directamente a la acción de un activador. Esto no es necesariamente previsible, puesto que se ha descrito que las regiones ricas en genes tienden a situarse de forma no aleatoria fuera del territorio cromosómico, independientemente de la actividad génica (Gilbert et al., 2004). Esto plantea la posibilidad de que el posicionamiento génico ligado a la actividad transcripcional pudiera estar condicionado por la localización en regiones cromosómicas amplias, y no por un reposicionamiento de dianas por parte de un activador.

Los estudios realizados en este trabajo de tesis evidencian que el reposicionamiento génico sí puede ser dependiente de un activador y se basa en dos aspectos: a) en ausencia de HNF1α, se observa un reposicionamiento específico de genes diana de HNF1α en dos tejidos diferentes, hígado (*Cyp2j5*) e islote (*Kif12*), pero no de cuatro genes control independientes de este activador (*Actb,*

Ly9, Nanog y *HNF1β*) respecto a dominios nucleares ricos en RNA polimerasa II y determinadas modificaciones de histona (ver Fig.4 y 5 de la segunda publicación en revisión en el J.Cell Biology) b) se ha documentado que existe un reposicionamiento selectivo para un locus HNF1α-dependiente empleando otro punto de referencia que no conlleva el análisis de dominios subnucleares. En particular, se estudiaron por doble FISH las distancias relativas entre el locus de *Cyp2j5* y dos clones adyacentes que mapan una región desierta de genes, y por lo tanto inactiva. Pese a la gran proximidad entre los 3 clones y estar equidistantes en el cromosoma (unas 20 pb entre clon y clon), el locus de *Cyp2j5,* activo en hepatocitos, está más alejado de su clon inmediatamente adyacente e inactivo que los dos clones inactivos y también adyacentes. Sin embargo estas diferencias desaparecen en los hepatocitos *Hnf1α*$^{-/-}$ donde *Cyp2j5* está silenciado, sugiriendo que el estado transcripcional dependiente de HNF1α de *Cyp2j5* influye en la posición del locus respecto al resto del cromosoma (ver Fig.6 de la segunda publicación en revisión en el J.Cell Biology). Este último hallazgo es importante, porque descarta que el aparente reposicionamiento sea debido a una reconfiguración de la estructura nuclear en células *Hnf1α*$^{-/-}$.

Existe un código de histona en el espacio nuclear?

Hemos demostrado que las modificaciones de histona se distribuyen de forma no aleatoria en el espacio nuclear formando dominios en gran medida no solapantes con potencialmente diferentes funciones.

Interesantemente, la marca H3-Lys27me3 no tiende a colocalizar ni con marcas activadoras como H3-Lys4me2, ni con marcas represoras como H3-Lys9me3, H3-Lys27me1 o H3-Lys27me2. Sin embargo colocaliza con H3-Lys9me2, sugiriendo que las modificaciones de histona se distribuyen en el núcleo formando subdominios ricos en una combinación determinada de marcas de histona. La localización de un locus en un subdominio rico en una combinación de marcas de histona podría tener repercusión en el estado transcripcional del locus. Hemos confirmado que los genes dependientes de HNF1α inactivos en ausencia de HNF1α están localizados selectivamente en dominios ricos en H3-Lys27me3 pero no ricos en H3-Lys9me3 o H3-Lys4me2. Desgraciadamente, el anticuerpo contra H3-Lys9me2 del que disponíamos no resistía el proceso de inmuno-FISH y por lo tanto no pudimos ampliar el estudio del posicionamiento dependiente de HNF1α respecto a determinadas combinaciones de modificaciones de histona.

La distribución claramente más periférica y perinucleolar de la trimetilación en H3-Lys27, frente a la distribución más interna de la dimetilación en H3-Lys4 y la RNA polimerasa II es interesante teniendo en cuenta estudios previos que asocian

la represión génica con una localización periférica y perinucleolar del locus, mientras que la internalización del locus correlaciona con actividad transcripcional (Kosak et al., 2002;Kosak and Groudine, 2004;Zink et al., 2004). Es posible por lo tanto que los dominios represivos referidos en estudios previos en base a una definición puramente radial, puedan estar más específicamente relacionados con la existencia de dominios represores ricos en determinadas marcas de histona

En este trabajo de tesis, hemos ampliado el concepto de reposicionamiento génico respecto a dominios ricos en RNA polimerasa II dependiendo de la actividad génica (Osborne et al., 2006; Ragozcy et al., 2006) y hemos demostrado que HNF1α induce el reposicionamiento de sus genes diana de un dominio rico en H3-Lys27me3 a un dominio rico en H3-Lys4me2. Estos cambios están en concordancia con las modificaciones observadas localmente por inmunoprecipitación de cromatina, lo que sugiere que existe una representación espacial y funcional de las marcas de histona en el núcleo.

La resolución de la microscopía óptica y el uso de BACs limita el estudio del reposicionamiento dependiente de activador.

A pesar de la asociación específica de los loci dependientes de HNF1α con dominios ricos en RNA polimerasa II y metilación de histonas en función de la actividad génica, esta correlación no es perfecta. Aunque somos capaces de diferenciar dos BACs adyacentes separados de 178 kb de centro a centro, existe algún precedente de reposicionamientos diferenciales de loci sensiblemente más pequeños (Zink et al,2004). Nuestros BACs suelen contener genes independientes de HNF1α situados en las proximidades del gen problema, por lo que el estado transcripcional de los genes vecinos puede influir en el análisis del posicionamiento de un determinado locus en el núcleo, disminuyendo nuestra capacidad para observar un efecto diferencial en ratones control y *Hnf1*$\alpha^{-/-}$.

Por otro lado, la transcripción es un fenómeno discontinuo, de manera que no todos los alelos están siempre transcribiéndose. A mayor tasa de transcripción, mayor es la probabilidad de encontrar el locus asociado con un dominio RNA polimerasa II (Osborne et al., 2004;Wijgerde et al., 1995). Por lo tanto, a pesar de ser potencialmente activo un gen HNF1α-dependiente en células control, podemos encontrar los loci no asociados con RNA polimerasa II.

Teniendo en cuenta todas estas limitaciones, es previsible que el reposicionamiento dependiente de HNF1α sea más evidente que lo mostrado en este estudio.

Modelo para integrar la existencia de cambios locales en la cromatina y reposicionamiento inducible por HNF1α.

La cromatina ha demostrado ser una estructura altamente dinámica en el núcleo. Seguimientos en levadura y Drosophila del movimiento de un locus marcado con una proteína de fluorescencia GFP han mostrado que la cromatina se desplaza de forma aparentemente errática en el espacio nuclear pero con una cierta limitación (Heun et al., 2001;Vazquez et al., 2001). Alcanza una distancia más o menos importante formando un círculo de acción (Heun et al., 2001;Vazquez et al., 2001). El radio de confinamiento depende de la localización y estado conformacional de la fibra de cromatina. Se ha visto que el posicionamiento cerca de la periferia nuclear o en dominios represores, tales como la heterocromatina constitutiva, reducen mucho la movilidad del locus (Chubb and Bickmore, 2003;Heun et al., 2001).

Por otra parte, otro tipo de estudios han indicado que la acetilación de las histonas aumenta la flexibilidad de la fibra de cromatina, mientras que corepresores, tales como HP1α o PcG, la compactan e inmovilizan (Francis et al., 2004;Krajewski and Becker, 1998;Shogren-Knaak et al., 2006). Así pues, proponemos que las modificaciones de cromatina (acetilación y metilación de H3-Lys4) inducidas por HNF1α localmente en sus genes diana aumentarían la flexibilidad de la fibra de cromatina y por lo tanto la movilidad del locus, favoreciendo su extrusión (*looping*) de zonas de cromatina más condensadas y ricas en marcas represoras como H3-Lys27me3. Este aumento de la movilidad del locus, aumentaría la probabilidad de encuentro con dominios ricos en RNA polimerasa II. La interacción entre el complejo de RNA polimerasa II y los coactivadores unidos al locus podría estabilizar el conjunto y aumentar el tiempo de residencia del locus en el dominio RNA polimerasa II, con la subsecuente transcripción. Por el contrario, en ausencia de HNF1α, la cromatina hipoacetilada y rica en H3-Lys27me3 se compactaría y perdería movilidad, quedándose anclada en dominios ricos en H3-Lys27me3 en el territorio cromosómico. (ver modelo).

Concluyendo, el análisis de la función in vivo del factor de transcripción HNF1α permite integrar tres niveles fundamentales de regulación de la transcripción, la secuencia primaria lineal de DNA, la cromatina y los dominios nucleares. Este trabajo no sólo aporta novedades sobre el funcionamiento de un activador transcripcional que regula un fenotipo epitelial diferenciado, sino que también aporta nuevas perspectivas sobre la comprensión de una enfermedad genética, la diabetes tipo MODY. De este modo, demuestra que una célula beta MODY3 es una célula en que genes importantes para el correcto funcionamiento y

desarrollo de la célula beta están apagados y deslocalizados a dominios represores ricos en H3-Lys27me3.

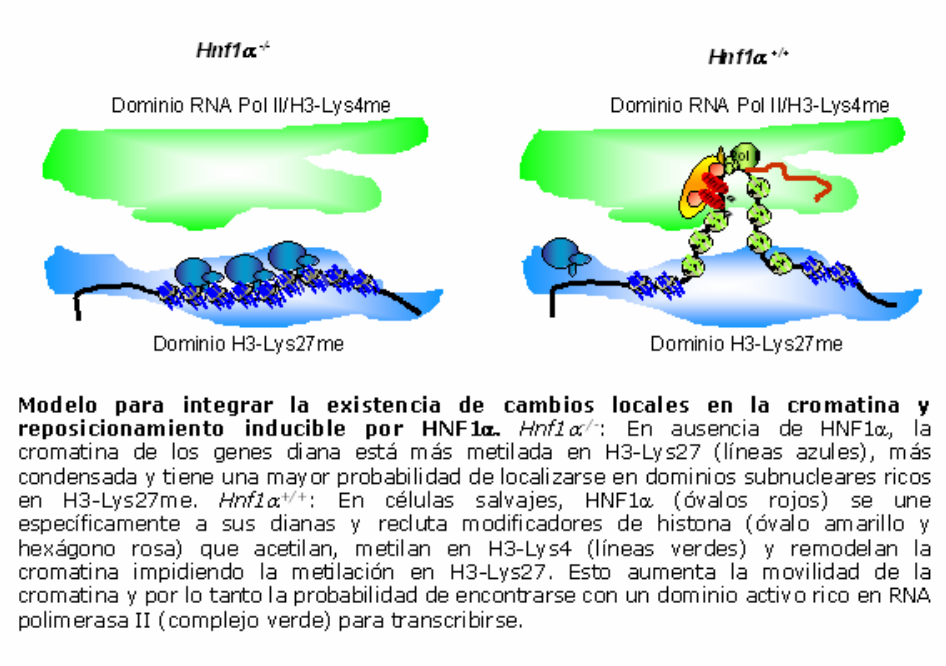

Modelo para integrar la existencia de cambios locales en la cromatina y reposicionamiento inducible por HNF1α. *Hnf1α*$^{-/-}$: En ausencia de HNF1α, la cromatina de los genes diana está más metilada en H3-Lys27 (líneas azules), más condensada y tiene una mayor probabilidad de localizarse en dominios subnucleares ricos en H3-Lys27me. *Hnf1α*$^{+/+}$: En células salvajes, HNF1α (óvalos rojos) se une específicamente a sus dianas y recluta modificadores de histona (óvalo amarillo y hexágono rosa) que acetilan, metilan en H3-Lys4 (líneas verdes) y remodelan la cromatina impidiendo la metilación en H3-Lys27. Esto aumenta la movilidad de la cromatina y por lo tanto la probabilidad de encontrarse con un dominio activo rico en RNA polimerasa II (complejo verde) para transcribirse.

Estos estudios plantean preguntas importantes respecto al mecanismo de movilidad de la cromatina en este modelo. ¿Depende de procesos activos dependientes de energía o de algún motor tipo la matriz nuclear y/o el nucleoesqueleto? ¿Es una causa o consecuencia de la actividad transcripcional? ¿Es un proceso dirigido o estocástico? ¿Son las marcas de histona presentes en los nucleosomas realmente las que inducen la relocalización del locus, o es la relocalización del locus a subdominios ricos en marcas de histona necesaria para la metilación del locus?

El núcleo se está revelando como el gran organizador de la célula que puede influir en el desarrollo, el mantenimiento de la identidad y el correcto funcionamiento celular. Hasta el punto que conocer el estado del núcleo será conocer el estado de la célula y por lo tanto su patología.

CONCLUSIONES

Las principales conclusiones de este trabajo son:

1.- La función de HNF1α en la célula beta tiene autonomía celular, puede ser parcialmente rescatada en células beta diferenciadas adultas y es altamente dependiente de la dosis génica.

2.- El reposicionamiento génico es un fenómeno localizado y dependiente de un activador.

3.- Las modificaciones de cromatina inducidas localmente por HNF1α tienen una representación funcional en el espacio nuclear. El reposicionamiento de genes activos a dominios nucleares ricos en RNA polimerasa II implica a su vez un reposicionamiento entre dominios subnucleares ricos en las mismas modificaciones de histona que se encuentran localmente al nivel de la cromatina de los genes implicados.